cmgh
CELLULAR AND MOLECULAR GASTROENTEROLOGY AND HEPATOLOGY

ORIGINAL RESEARCH

A Mitochondrial DNA Variant Elevates the Risk of Gallstone Disease by Altering Mitochondrial Function

Dayan Sun,[1,2,#] Zhenmin Niu,[3,#] Hong-Xiang Zheng,[2,4,#] Fei Wu,[1] Liuyiqi Jiang,[1] Tian-Quan Han,[5] Yang Wei,[1] Jiucun Wang,[1,2,6,7,*] and Li Jin[1,2,6,7,*]

[1]State Key Laboratory of Genetic Engineering, School of Life Sciences, and Human Phenome Institute, Fudan University, Shanghai, China; [2]Collaborative Innovation Center for Genetics and Development, Fudan University, Shanghai, China; [3]Shanghai-MOST Key Laboratory of Health and Disease Genomics, Chinese National Human Genome Center at Shanghai and Shanghai Academy of Science and Technology, Shanghai, China; [4]Ministry of Education Key Laboratory of Contemporary Anthropology, Department of Anthropology and Human Genetics, School of Life Sciences, Fudan University, Shanghai, China; [5]Shanghai Institute of Digestive Surgery, Department of Surgery, Ruijin Hospital, Shanghai Jiaotong University School of Medicine, Shanghai, China; [6]Research Unit of Dissecting the Population Genetics and Developing New Technologies for Treatment and Prevention of Skin Phenotypes and Dermatological Diseases (2019RU058), Chinese Academy of Medical Sciences, Shanghai, China; and [7]Taizhou Institute of Health Sciences, Fudan University, Taizhou, China

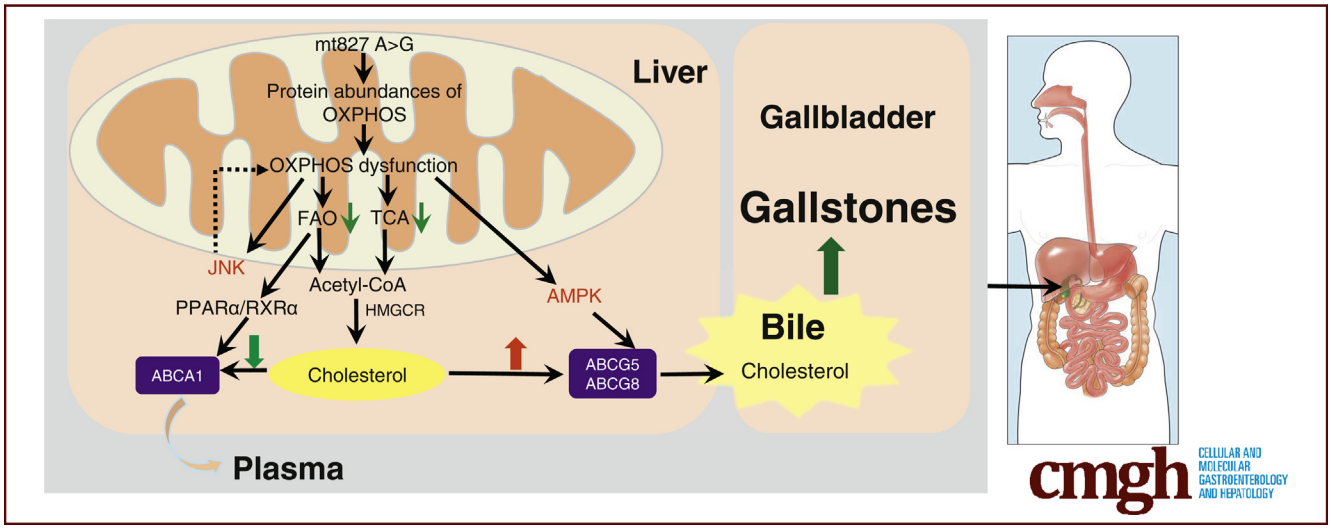

SUMMARY

Mitochondrial DNA 827A>G induces aberrant mitochondrial function and abnormal cholesterol transport through the transporter ABCG5/8 (ATP binding cassette subfamily G member 5/8) via activation of the AMPK signaling pathway, which increases the formation of gallstones.

BACKGROUND AND AIMS: Gallstone disease (cholelithiasis) is a cholesterol-related metabolic disorders with strong familial predisposition. Mitochondrial DNA (mtDNA) variants accumulated during human evolution are associated with some metabolic disorders related to modified mitochondrial function. The mechanistic links between mtDNA variants and gallstone formation need further exploration.

METHODS: In this study, we explored the possible associations of mtDNA variants with gallstone disease by comparing 104 probands and 300 controls in a Chinese population. We constructed corresponding cybrids using trans-mitochondrial technology to investigate the underlying mechanisms of these associations. Mitochondrial respiratory chain complex activity and function and cholesterol metabolism were assessed in the trans-mitochondrial cell models.

RESULTS: Here, we found a significant association of mtDNA 827A>G with an increased risk of familial gallstone disease in a Chinese population (odds ratio [OR]: 4.5, 95% confidence interval [CI]: 2.1–9.4, $P=1.2\times10^{-4}$). Compared with 827A cybrids (haplogroups B4a and B4c), 827G cybrids (haplogroups B4b and B4d) had impaired mitochondrial respiratory chain complex activity and function and activated JNK and AMPK signaling pathways. Additionally, the 827G cybrids showed disturbances in cholesterol transport and accelerated development of gallstones. Specifically, cholesterol transport through the transporter ABCG5/8 was increased via activation of the AMPK signaling pathway in 827G cybrids.

CONCLUSIONS: Our findings reveal that mtDNA 827A>G induces aberrant mitochondrial function and abnormal cholesterol transport, resulting in increased occurrence of gallstones. The results provide an important biological basis for the clinical

diagnosis and prevention of gallstone disease in the future. *(Cell Mol Gastroenterol Hepatol 2021;11:1211–1226; https://doi.org/10.1016/j.jcmgh.2020.11.015)*

Keywords: mtDNA 827A>G; Gallstone Disease; Mitochondrial Function; Cholesterol Transport; Chinese Population.

Gallstone disease (cholelithiasis) is a common disease that is related to abnormal metabolism of lipids. Most gallstones are caused by supersaturation of cholesterol in the bile that leads to cholesterol crystallization and stone nidus formation, and <10% of stones are black and brown pigment stones.[1] The etiology of gallstone disease is multifactorial; age, sex, pregnancy, diet (macronutrients, alcohol, and coffee), and other factors are involved.[2,3] Moreover, the significant familial predisposition[4] and ethnic differences in prevalence[5] of this disease indicate the potential influences of genetic factors. A recent analysis of U.S. populations suggested that genetic factors are responsible for at least 30% of gallstone disease cases,[6] and the highest prevalence of gallstones is observed in Native Americans (>70% among women).[7]

Previous genome-wide association studies have identified a variant of the hepatobiliary cholesterol transporter ATP binding cassette subfamily G member 8 (*ABCG8*) as the most frequent genetic risk factor in gallstone disease patients.[8] Another study has demonstrated that the lithogenic genes ATP binding cassette subfamily G member 5 (*ABCG5*) and *ABCG8*, as well as *UGT1A1* (UDP glucuronosyltransferase family member A1), may cause gallstone formation.[9] Moreover, rare mutations in ATP binding cassette subfamily B member 4 (*ABCB4*), ATP binding cassette subfamily B member 11 (*ABCB11*), *CFTR* (cystic fibrosis transmembrane conductance regulator), and *CYP7A1* (cytochrome P450 family 7 subfamily A member 1) may promote gallstone formation by altering bile composition.[10] Interestingly, gallstone formation is frequent in patients with diabetes. One group has clarified that insulin resistance elevates biliary cholesterol secretion by upregulating ABCG5 and ABCG8 via dysregulation of the transcription factor FOXO1 (forkhead box protein O1) in hepatocytes.[11] In addition, activation of the nuclear receptor LXR (liver X receptor) can enhance biliary cholesterol secretion by increasing ABCG5 and ABCG8 levels in hepatocytes.[12] Collectively, these findings reveal that nuclear variants indeed contribute to gallstone formation to some extent.

Mitochondria play important roles in the metabolism of glucose and lipids by conducting oxidative phosphorylation (OXPHOS) and producing adenosine triphosphate (ATP).[13,14] Thus, mitochondrial DNA (mtDNA) abnormalities can influence the production of ATP and in turn contribute to the etiologies of common metabolic diseases. Type 2 diabetes is a classic metabolic disease that has been linked to mtDNA variants, such as 3310C>T, 3394T>C and 3243A>G.[15–17] Furthermore, mtDNA variants have been identified as being responsible for many metabolic defects, including hypertension and dyslipidemia.[18–20] Notably, mitochondrial function has been found to be associated with beta-oxidation and OXPHOS in fat and steroid metabolism.[21] In addition, observations of maternal bias in the maternal transmission of gallstone disease have suggested that mtDNA variants are associated with familial gallstone disease.[22] Therefore, we hypothesized that mtDNA variants may contribute to the occurrence of gallstones, which are manifestations of lipid metabolic abnormalities.

In this study, we explored the possible associations between mtDNA variants and gallstone disease by comparing 104 probands and 300 controls in a Chinese population. The results showed a strong association of gallstone disease with mtDNA haplogroup B4b′d′e′j. A variant defining haplogroup B4b′d′e′j, 827A>G, in mitochondrial 12S ribosomal RNA (rRNA) emerged as the most likely candidate responsible for the observed association. Thus, we investigated the pathological mechanism of gallstone disease associated with 827A>G by using transmitochondrial technology in this study. Mitochondrial respiratory chain complex activity and function, and cholesterol metabolism were assessed in the transmitochondrial cell models. Our findings revealed that mtDNA 827A>G induced aberrant mitochondrial function and abnormal cholesterol transport, resulting in increased occurrence of gallstones.

Results

Associations of mtDNA Variants With Gallstone Disease

We first investigated the relationships between mtDNA variants and gallstone disease in a Chinese population. DNA samples from 104 unrelated probands (mean age 44.9 years; range, 19–81 years) with confirmed gallstone disease (cholelithiasis) and a total of 300 unrelated individuals (mean age 64 years; range, 50–86 years) were collected from the Greater Shanghai Area. The average total cholesterol and triglyceride concentrations of the patients were 4.41 (normal range, 2.8–5.17) mmol/L and 1.67 (normal range, 0.56–1.7) mmol/L, respectively. We sequenced the mtDNA HVS1 regions of the 104 patients and 300 controls, and the results showed that 2 variants, 16217C ($P = .041$) and 16136C ($P = .007$), showed significantly higher frequencies in the cases than in the controls. Interestingly, both variants were mutations defining B4 haplogroup (ie, 16217C defined B4, and 16136C defined B4b1). The *P* values for the chi-square test and Fisher′s exact test of the

[#]Authors share co-first authorship.

Abbreviations used in this paper: **ABCB11, ATP binding cassette subfamily B member 11; ABCB4, ATP binding cassette subfamily B member 4; ABCG5, ATP binding cassette subfamily G member 5; ABCG8, ATP binding cassette subfamily G member 8; ATP, adenosine triphosphate; mtDNA, mitochondrial DNA; mRNA, messenger RNA; nDNA, nuclear DNA; OXPHOS, oxidative phosphorylation; rRNA, ribosomal RNA; SNP, single nucleotide polymorphism; TCA, tricarboxylic acid.**

Most current article

2352-345X
https://doi.org/10.1016/j.jcmgh.2020.11.015

Table 1. Association of mtDNA Haplogroups B4b′d′e′j With Gallstone Disease

	mtDNA Mutation and Haplogroup						
	16217C	16261	827G	499A	13942G	16136C	6413C
	B4	B4a	B4b′d′e′j	B4b	B4d	B4b1	—
Cases (n = 104)	20	5	15	11	4	11	8
%	19.23	4.81	14.42	10.58	3.85	10.58	7.69
Controls (n = 300)	34	15	11	11	0	11	3
%	11.33	5.00	3.67	3.67	0	3.67	1.00
P (χ^2)	.041	.938	1.2×10^{-4}	7.5×10^{-3}	6.4×10^{-4}	7.5×10^{-3}	2.3×10^{-4}
P (FET)	.046	>0.999	3.5×10^{-4}	.012	.004	.012	1.3×10^{-3}
OR	1.863	0.960	4.428	3.107	/	3.107	8.25
95% CI	1.02–3.38	0.34–2.71	2.08–9.44	1.35–7.13	/	1.35–7.13	2.68–25.3

NOTE. Probabilities of observed associations were calculated based on Pearson chi-square test, FET, and OR.
CI, confidence interval; FET, Fisher's exact test; OR, odds ratio.

associations between gallstone disease and the closely related polymorphisms are presented in Table 1. A 9-bp deletion at 8281–8289, the diagnostic marker of haplogroup B4′5, showed no association between the cases (n = 23 of 104) and the controls (n = 50 of 300) (P >0.05). In addition, the prevalence of B5, the sister group of B4, was not significantly different between the cases (n = 4 of 104) and controls (n = 12 of 300), further supporting the significance of haplogroup B4. Moreover, the mitochondrial whole genome results showed the variant 827A>G in mitochondrial 12S rRNA was the candidate most likely responsible for gallstone disease (Table 2).

Next, we explored the frequency differences of the mutations defining the subhaplogroups of B4 between cases and controls to identify the subhaplogroups most associated with gallstone disease. In the phylogenetic tree (Figure 1*A*) and median-joining network (Figure 1*B*) of haplogroup B4, we found that haplogroup B4b′d′e′j showed a higher odds ratio (4.428) and more significant *P* value (1.2×10^{-4}) (n = 15 of 104 patients and n = 11 of 300 controls) than the other haplogroups in B4 (B4, B4a, B4b1, and B4d), indicating that B4b′d′e′j was the haplogroup most likely associated with gallstone disease and that the variant harbored in this haplogroup might contribute to gallstone disease.

During the evolutionary history of modern humans, haplogroup B4 might have originated in East Asia approximately 40,000 years ago.[23,24] B4b′d′e′j arose from B4 with the mutations 827A>G (a variant in 12S rRNA) and 15535C>T (a synonymous mutation in CytB). Thus, we hypothesized that 827A>G might have a considerable effect on the etiology of gallstone disease. B2, a subhaplogroup of B4b′d′e′j, was a founder haplogroup and expanded in the

Table 2. Analysis of Whole Mitochondrial Genome of the 4 B4b′d′e′j Individuals

		Patients					
Position	CRS	P13	P46	P74	P89	Region	AA Change
827	A	G[a]	G[a]	G[a]	G[a]	12S rRNA	—
4820	G	A[a]	A[a]	A[a]	G	ND2	None
5292	T	T	T	T	C[a]	ND2	Ser > Arg
6023	G	A[a]	A[a]	G	G	COXI	None
6216	T	C[a]	C[a]	T	T	COXI	None
6413	T	C[a]	C[a]	T	T	COXI	None
13590	G	A[a]	A[a]	A[a]	G	ND5	None
13801	A	A	A	A	G[a]	ND5	Thr > Ala
13942	A	A	A	A	G[a]	ND5	Thr > Ala
14587	A	A	A	G[a]	A	ND6	None
15315	C	C	C	C	T[a]	Cytb	Ala > Val
15535	C	T[a]	T[a]	T[a]	T[a]	Cytb	None
15930	G	G	G	G	A[a]	tRNA-Thr	—

AA, amino acid; CRS, Cambridge Reference Sequence; rRNA, ribosomal RNA; tRNA, transfer RNA.
[a]Presents the site is mutant.

Americas after the Last Glacial Maximum (approximately 20,000 years ago).[25,26] Thus, the frequencies of 827A>G B4 carriers were higher in Native Americans (14%–44%) than in East Asians (2%–8%) (Figure 1*C*; Supplementary Table 1). Interestingly, we found that the prevalence of gallstone disease was also significantly higher in Native Americans (14%–35%) than in East Asians (3%–12%) ($P = .002$, t test), suggesting the possible role of B4b′d′e′j in gallstone disease.

In addition, conservation analysis of vertebrates showed that 827A>G was generally conserved among all the species tested (Figure 1*D*), indicating that this adenosine might be

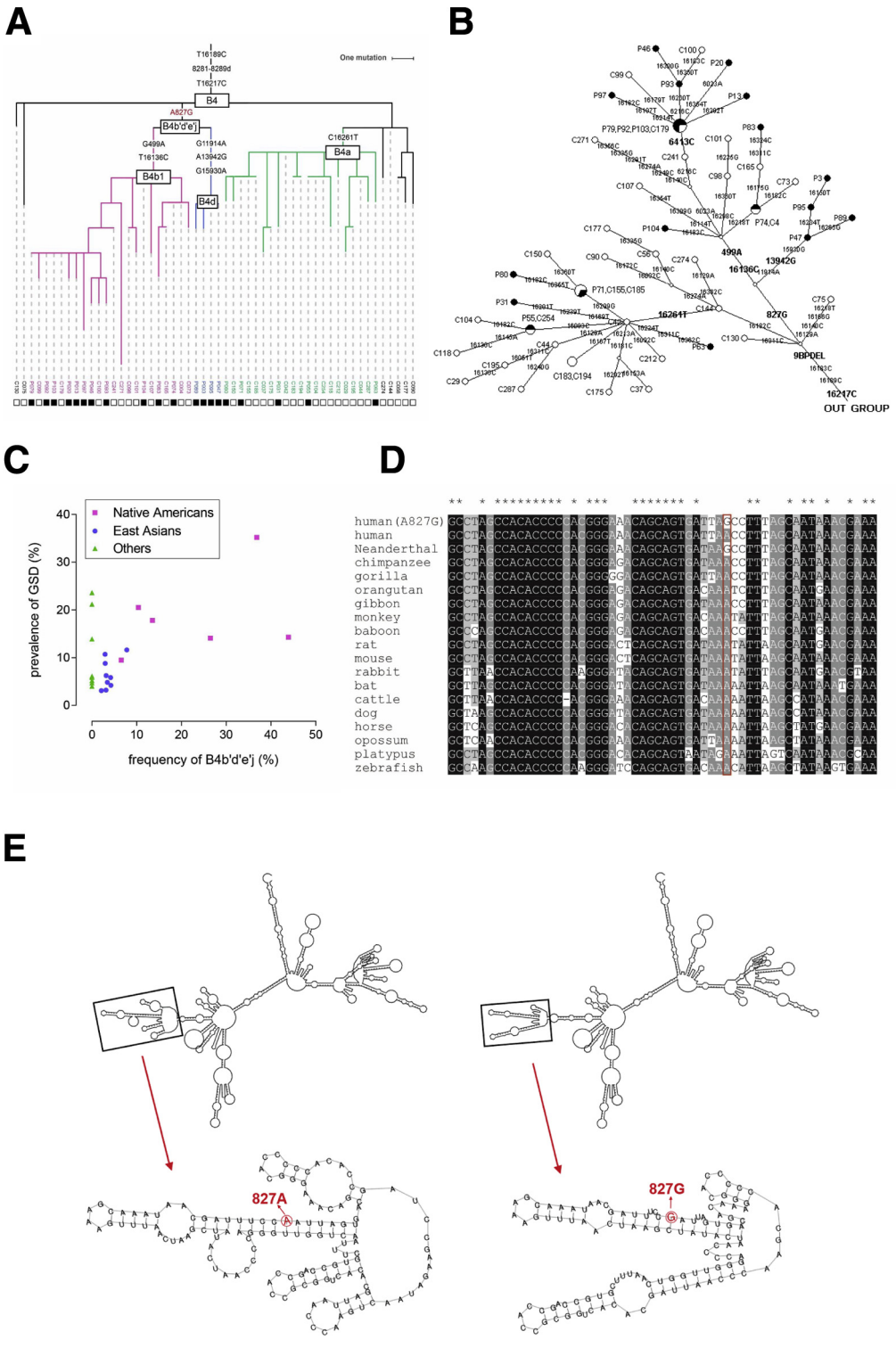

important in maintaining 12S rRNA function in different species and that mutations at this site are subject to purifying selection. We further predicted the RNA structure of 12S rRNA with or without 827A>G using the RNAfold program implemented in the Vienna RNA Package 2.0 (Figure 1*E*).[27] The results indicated that the 827A>G variant in 12S rRNA might change the nearby loop structure.

In summary, we found that the 12S rRNA variant 827A>G harbored in haplogroup B4b′d′e′j might affect mitochondrial function and in turn affect the prevalence of gallstone disease.

The 827G Cybrids Exhibited Lower Respiratory Chain Complex Activity Than the 827A Cybrids

To analyze the effect of the 827A>G variant on the regulation of the mitochondrial respiratory chain complex, we constructed 2 groups of sister branch haplogroup cell models: 827A cybrids (B4a/B4c haplogroups) (n = 6), and 827G cybrids (B4b/B4d haplogroups) (n = 6) according to the mtDNA phylogenetic tree. First, to determine whether 827A>G affects mitochondrial respiratory chain complex activity, we evaluated the transcript levels of 12S rRNA and mtDNA-encoded OXPHOS genes in the 827A and 827G cybrids. The results illustrated that the RNA levels of 12S rRNA, ND4/4L, ND5, ND6, CO3, ATP6, and ATP8 were significantly higher in the 827A cybrids than in the 827G cybrids (Figure 2*A* and *C*). In addition, mitochondrial ribosomal small subunit transcript levels were lower in the 827G cybrids than in the 827A cybrids, consistent with the results of the transcriptomic gene expression analysis of all 30 mitochondrial ribosomal small subunits (Figure 2*A* and *B*). Moreover, nuclear DNA (nDNA)-encoding OXPHOS gene expression tended to be lower in the 827G cybrids than in the 827A cybrids (Figure 2*D*). However, the mtDNA copy number did not significantly differ in either cybrids or peripheral blood mononuclear cell samples between the 827A (n = 206) and 827G (n = 82) genotypes (Figure 2*E* and *F*).

We further determined the mtDNA-encoding and nDNA-encoding protein expression levels in the 827A and 827G cybrids. The results revealed that the expression levels of most of the proteins, especially the ND5 subunit, were lower in the 827G cybrids than in the 827A cybrids, which may have impaired the assembly of OXPHOS complex I (Figure 2*G* and *H*). This finding confirms that 12S rRNA plays important roles in the processes of mtDNA transcription and translation. Finally, we examined the activity of the 4 respiratory chain complexes, and the results showed that complex I activity relative to citrate synthase activity was significantly higher in the 827A cybrids than in the 827G cybrids (Figure 2*I*).

Collectively, these results indicated that the 827G cybrids had lower respiratory chain complex activity than the 827A cybrids.

Compared With the 827A Cybrids, the 827G Cybrids Presented Diminished Mitochondrial Function

To corroborate the effect of the 827A>G variant on the mitochondrial respiratory chain complex, we detected OXPHOS function in the 827A and 827G cybrids. The results showed that the total ATP content, basal mitochondrial respiration, and OXPHOS-driven mitochondrial respiration were significantly lower in the 827G cybrids than in the 827A cybrids (Figure 3*A* and *B*). However, reactive oxygen species (ROS) generation was increased by 50% in the 827G cybrids compared with 827A cybrids (Figure 3*C*), which may have further activated mitochondrial quality control protein expression and mitochondrial-nuclear signaling pathways. Thus, compared with the 827A cybrids, the 827G cybrids presented diminished mitochondrial OXPHOS function.

The Mitochondrial Protein Quality Control Response and Retrograde Signaling Pathways Were Activated in the 827G Cybrids

We further investigated whether the ROS increases caused by mitochondrial dysfunction activated the expression of mitochondrial quality control proteins. The results showed that the levels of CLPP and LONP1 were significantly higher in the 827G cybrids than in the 827A cybrids, suggesting that the 827G cybrids experienced ROS stress. Notably, the mitophagy-related protein PINK1 tended to be downregulated in the 827G cybrids compared with the 827A cybrids (Figure 4*A* and *B*). Consistent with this result, the messenger RNA (mRNA) expression levels of the mitophagy-associated genes *p62* and *LC3* also tended to be

Figure 1. (***See previous page***). **Association of mtDNA haplogroup B4b′d′e′j with gallstone disease.** (*A*) PhyloTree of B4 individuals among the cases and controls. Each square represents a haplogroup observed in this study. The filled squares represent the cases (marked with labels starting with P), and the open squares represent the controls (marked with labels starting with C). The inferred mutations are marked by short lines. Green represents mtDNA haplogroup B4a, pink represents mtDNA haplogroup B4b1, blue represents mtDNA haplogroup B4d, and black represents other subhaplogroups of mtDNA haplogroup B4. (*B*) Network of B4 individuals among the cases and controls. This median-joining network was reconstructed using NETWORK software. Each circle represents a haplogroup observed in this study. The size of the circle is proportional to the number of individuals carrying the haplotype. The filled circles represent the cases (marked with labels starting with P) and the open circles represent the controls (marked with labels starting with C). The root of the network is labeled as the Out group. The inferred mutations are marked on the lines connecting the haplogroups. (*C*) Scatterplot of the prevalence of gallstones and the frequency of mtDNA haplogroup B4b′d′e′j. The blue circles represent East Asians; the pink squares represent Native Americans; and the green triangles represent others, including Africans and Eurasians. (*D*) Conservation analysis of the mtDNA 827A>G variant in 12S rRNA. Blue and red indicate the 827 position with the A and G polymorphisms, respectively. (*E*) Secondary structure of the mtDNA 827A>G variant in 12S rRNA. (Left) Wild-type 12S rRNA; (right) 12S rRNA with the mtDNA 827A>G variant. The corresponding panels show enlargements of the regions of predicted secondary structures surrounding nucleotide position 827 (bold arrows with red circles).

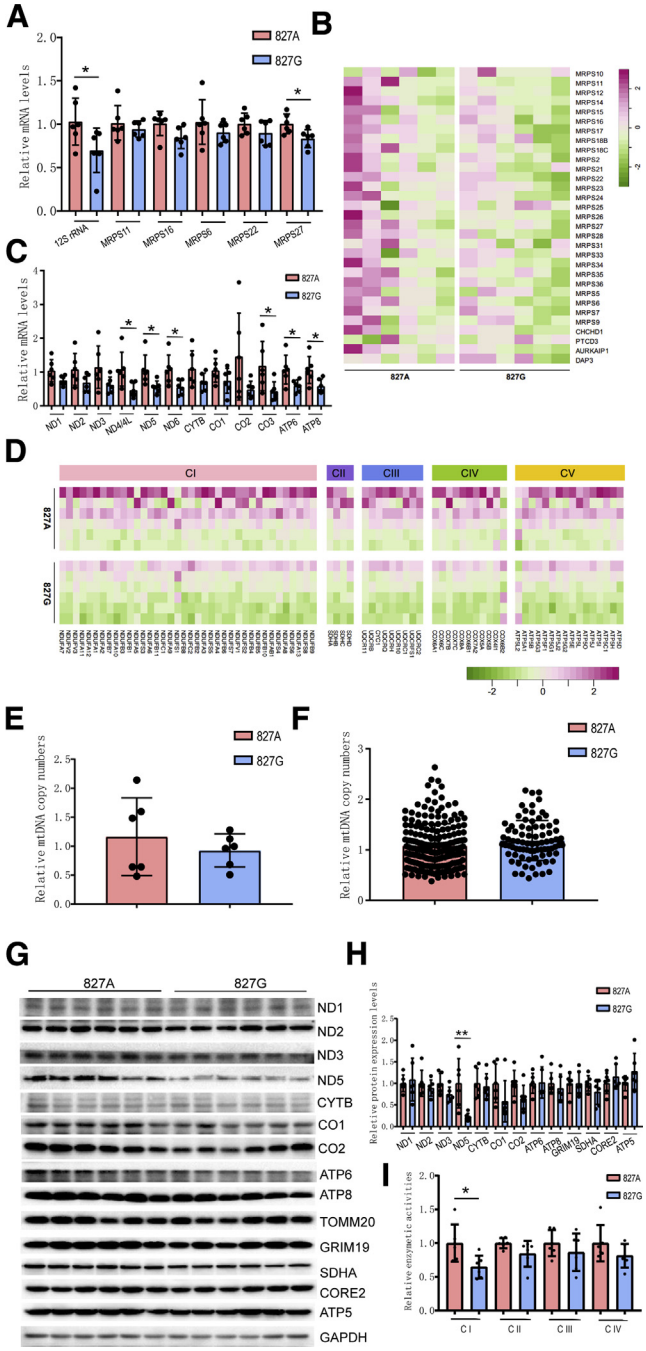

Figure 2. The 827G cybrids exhibited lower respiratory chain complex activity than the 827A cybrids. (*A*) Mitochondrial 12S rRNA and ribosomal protein small subunit–related gene transcript levels in the 827A (n = 6) and 827G (n = 6) cybrids. The relative mitochondrial ribosomal protein transcript levels in the 827G cybrids were normalized to the levels in the 827A cybrids. (*B*) Heatmaps of all the mitochondrial ribosomal protein small subunit–related gene levels between the 827A (n = 6) and 827G (n = 6) cybrids. The gradual color change from red to green represents the expression change from upregulation to downregulation. (*C*) Mitochondrial RNA levels in the 827A (n = 6) and 827G (n = 6) cybrids. The relative mitochondrial RNA levels in the 827G cybrids were normalized to the levels in the 827A cybrids. ND4/4 L, ND4, and ND4L. (*D*) Heatmaps of OXPHOS nDNA-encoded gene expression between the 827A (n = 6) and 827G (n = 6) cybrids. (*E*) MtDNA copy number levels of the 827A (n = 6) and 827G (n = 6) cybrids. The relative mtDNA copy number levels in the 827G cybrids were normalized to the levels in the 827A cybrids. (*F*) MtDNA copy number levels of the peripheral blood mononuclear cell samples of the 827A (n = 206) and 827G (n = 82) genotypes. The relative mtDNA copy number levels for the 827G genotype were normalized to the levels for the 827A genotype. (*D*) Immunoblot analysis of the levels of OXPHOS mtDNA-encoded and nDNA-encoded proteins in whole-cell extracts of the 827A (n = 6) and 827G (n = 6) cybrids. TOMM20 and ACTIN were used as loading controls for the mtDNA-encoded and nDNA-encoded proteins, respectively. (*E*) Quantified signal intensities of the OXPHOS mtDNA-encoded protein bands/TOMM20 bands and nDNA-encoded protein bands/ACTIN bands. The levels of proteins in the 827G cybrids were normalized to those in the 827A cybrids (the mean value for cybrids 827A was set to 1). (*F*) The enzymatic activity levels of mitochondrial complexes I, II, III, and IV and of citrate synthase were measured in mitochondria isolated from 827A (n = 6) and 827G (n = 6) cybrids. The enzymatic activity levels in the 827G cybrids were normalized to those in the 827A cybrids. The data are presented as the mean ± SD from at least 3 independent tests per experiment. *$P < .05$; **$P < .01$.

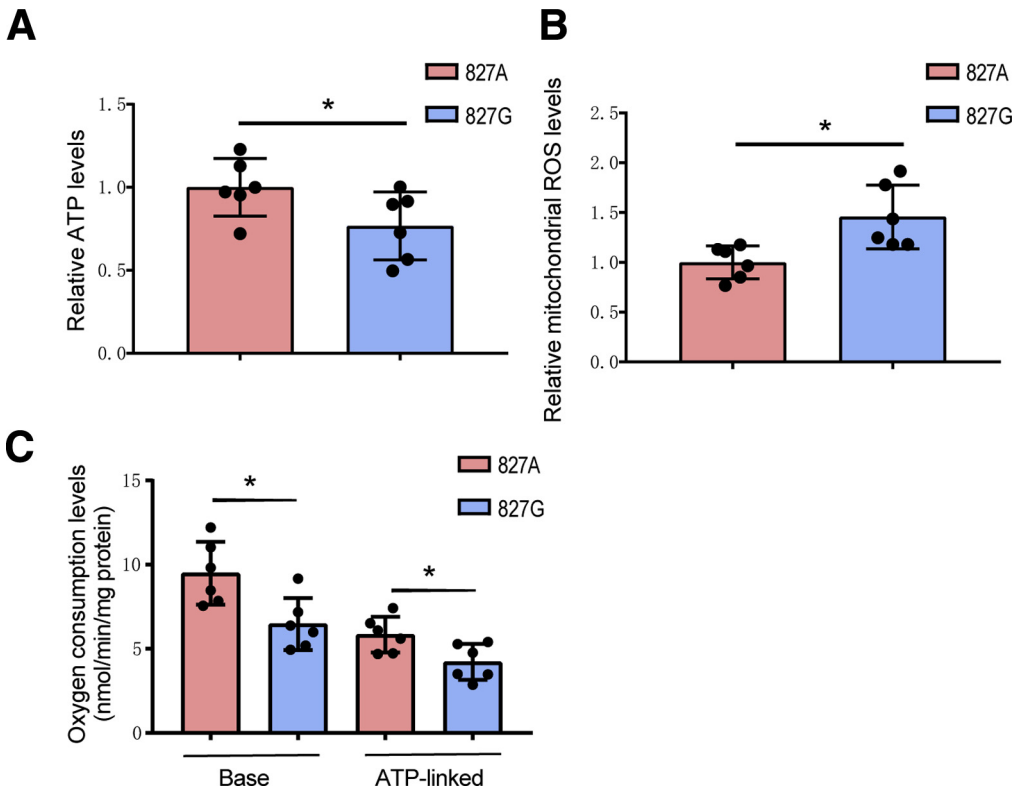

Figure 3. The 827G cybrids presented diminished mitochondrial function compared with the 827A cybrids. (*A*) Total ATP content was measured in the 827A (n = 6) and 827G (n = 6) cybrids. The ATP levels in the 827G cybrids were normalized to those in the 827A cybrids. (*B*) Mitochondrial ROS levels were determined in the 827A (n = 6) and 827G (n = 6) cybrids. The mitochondrial ROS levels in the 827G cybrids were normalized to those in the 827A cybrids. (*C*) Mitochondrial respiratory capacity was determined in the 827A (n = 6) and 827G (n = 6) cybrids. Oligomycin (2.5 μg/mL) was added for measurement of coupled mitochondrial respiration. OXPHOS coupling respiration was calculated by subtracting the uncoupled component value from the total endogenous respiration value. The data are presented as the mean ± SD from at least 3 independent tests per experiment. *$P < .05$.

lower in the 827G cybrids than in the 827A cybrids (Figure 4*C*). These findings suggest that deficient mitophagy in the 827G cybrids hampered the cybrids to cope with stress.

As altered mitochondrial ROS generation has been found to be related to modification of many mitochondria-to-nucleus retrograde signaling pathways, we examined several major signaling pathways in the 827A and 827G cybrids. The results indicated that the JNK and AMPK pathways, which are related to OXPHOS gene expression and catabolism, respectively, were activated in the 827G cybrids (Figure 4*D* and *E*). In addition, the nuclear receptor RXRα, which mediates the biological effects of OXPHOS gene activation, was significantly downregulated in the 827G cybrids compared with the 827A cybrids (Figure 4*F* and *G*). Thus, the results suggested that OXPHOS complex capacity was decreased and that catabolism was increased for energy compensation in the 827G cybrids.

Abnormal Lipid Metabolism and Cholesterol Transport Processes Occurred in the 827G Cybrids

We further investigated whether abnormal lipid metabolism occurred in the 827G cybrids and found that the mRNA expression levels of fatty acid metabolism–related genes (*CPT1A*, *CPT1B*, *VLCAD*, *ACOX1*, and *PPARα*) were significantly downregulated in the 827G cybrids compared with the 827A cybrids (Figure 5*A*). In addition, the protein levels of *CPT1A* and *PPARα* were significantly decreased in the 827G cybrids compared with the 827A cybrids (Figure 5*B* and *C*). The results indicated that long-chain fatty acid transport and fatty acid β-oxidation processes were aberrant in the 827G cybrids.

Additionally, we examined the gene expression levels of the main enzymes in the metabolic processes of glycolysis and the tricarboxylic acid (TCA) cycle. The results illustrated that the gene expression of the key glycolysis enzymes PFKL and LDHA and the key TCA cycle enzymes PDHA, IDH, SDHA, FH, and MDH1 were evidently downregulated in the 827G cybrids compared with 827A cybrids. Downregulation of glycolysis in the 827G cybrids might have reduced the levels of the substrate for TCA and cholesterol synthesis, acetyl coenzyme A, thus hampering the TCA cycle and decreasing ATP generation. In addition, the levels of acetyl coenzyme A used for cholesterol synthesis might have decreased due to excessive accumulation of cholesterol in gallstones (Figure 5*D* and *E*). However, cholesterol synthesis showed no significant difference between the 827A and 827G cybrids (Figure 5*F*). The protein level and enzymatic activity of the

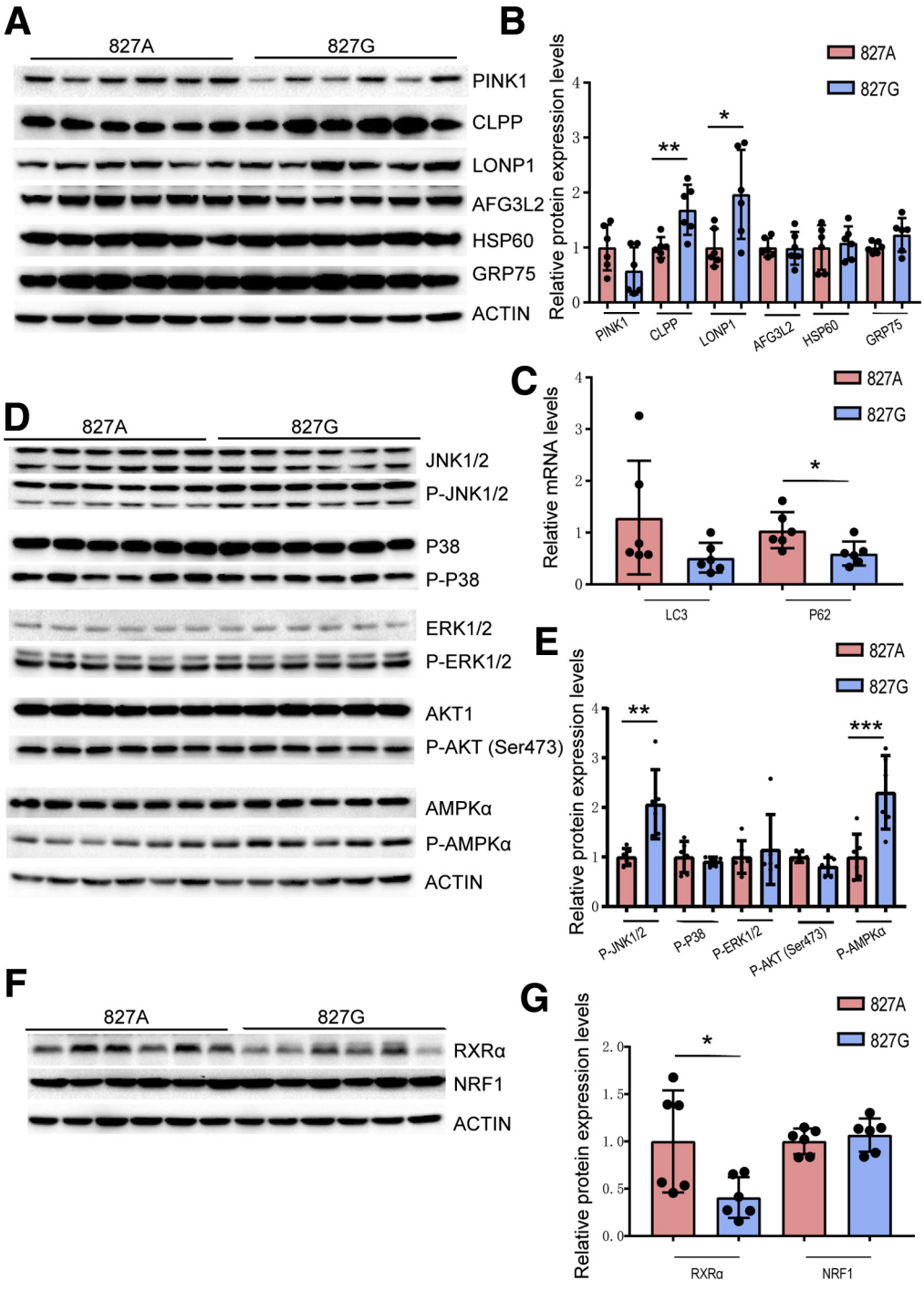

Figure 4. The mitochondrial protein quality control response and retrograde signaling pathways were activated in the 827G cybrids. (*A*) Representative Western blot of the mitochondrial quality control proteins PINK1, CLPP, LONP1, AFG3L2, HSP60, GRP75, and VDAC in whole-cell extracts from the 827A (n = 6) and 827G (n = 6) cybrids. ACTIN was used as a loading control. (*B*) Quantified signal intensities of all the target protein bands/ACTIN bands. The levels of proteins in the 827G cybrids were normalized to those in the 827A cybrids (the mean value for the 827A cybrids was set to 1). (*C*) Mitophagy associated gene expression in the 827A (n = 6) and 827G (n = 6) cybrids. The relative gene expression in the 827G cybrids was normalized to the expression in the 827A cybrids. (*D*) Representative Western blot of the relative phosphorylation of JNK, P38, ERK, AKT, and AMPK in whole-cell extracts from the 827A (n = 6) and 827G (n = 6) cybrids. ACTIN was used as a loading control. The levels of proteins in the 827G cybrids were normalized to those in the 827A cybrids. (*E*) Quantified signal intensities of all the target protein bands/ACTIN bands. The levels of proteins in the 827G cybrids were normalized to those in the 827A cybrids (the mean value for the 827A cybrids was set to 1). (*F*) Representative Western blot of the mitochondrial retrograde signaling mediators NRF1 and RXRα in whole-cell extracts from the 827A (n = 6) and 827G (n = 6) cybrids. ACTIN was used as a loading control. (*G*) Quantified signal intensities of the NRF1 and RXRα protein bands/ACTIN bands. The levels of proteins in the 827G cybrids were normalized to those in the 827A cybrids (the mean value for 827A cybrids was set to 1). The data are presented as the mean ± SD from at least 3 independent tests per experiment. *$P < .05$; **$P < .01$; ***$P < .001$.

rate-limiting enzyme of cholesterol synthesis, HMGCR, also did not differ between the 827A and 827G cybrids (Figure 5*G*–*I*). As expected, the total cellular cholesterol levels were similar between the 827A and 827G cybrids (Figure 5*J*–*L*).

Next, we focused on the transport processes in the 827A cybrids and 827G cybrids. The expression of the transporter ABCA1, which mediates cholesterol efflux to peripheral blood, was downregulated in the 827G cybrids compared with the 827A cybrids; however, the expression of the transporter ABCG5/8, which mediates cholesterol efflux to bile and the gallbladder, was upregulated in the 827G cybrids compared with the 827A cybrids (Figure 5*M* and *N*).

Because evidence has shown that hypoxic conditions contribute to the formation of gallstones,[28] we further evaluated whether hypoxia promoted the formation of gallstones in 827G cybrids. The cybrids were cultured in 1% O_2 for 36 hours, and the results showed that the levels of the transporter ABCG5/8 increased dramatically in the 827G cybrids compared with the 827A cybrids, partly dependent on the HIF1α pathway (Figure 5*M* and *N*).

Taken together, our results showed that abnormal cholesterol transport, but not cholesterol synthesis, promoted gallstone formation in the 827G cybrids.

Discussion

In this study, we demonstrated a strong association of the mtDNA haplogroups B4b′d′e′j with gallstone disease in a Chinese population. Furthermore, mtDNA 827A>G, a highly conserved site in mitochondrial 12S rRNA defining the B4b′d′e′j haplogroups, induced aberrant mitochondrial function and elevated the occurrence of gallstones by inducing abnormal cholesterol transport through ABCG5/8 via activation of the AMPK signaling pathway.

Mitochondrial 12S rRNA plays an important role in the synthesis of mtDNA-encoded proteins, which may contribute to mitochondrial OXPHOS function.[29] The human mitochondrial ribosomal small subunit comprises mitochondrial 12S rRNA and 30 ribosomal proteins encoded by nDNA in eukaryotic cells.[30] Variants in the mitochondrial 12S rRNA genes, especially 827A>G, have been found to be associated with various diseases, such as cardiomyopathy,[31] nonsyndromic and aminoglycoside-induced hearing loss.[32,33] and age-related hearing loss in Chinese individuals.[34] However, the underlying mechanisms remain unknown and need further exploration.

The 143B osteosarcoma ρ0 cell line was the first mtDNA-deleted cell model successfully constructed[35] and has been widely used to study human evolution-related topics, such as mtDNA haplogroup function in East Asia[36] and high-altitude population adaptability.[37] In addition, many diseases, including diabetes,[38] osteoarthritis,[39] and hepatocellular carcinoma,[40] have been studied in this cell model. Therefore, we chose the 143B osteosarcoma ρ0 cell line in combination with 827A- and 827G-related haplogroups plasma for our research.

Notably, the mitochondrial complex I ND5 subunit, which plays a pivotal role in complex I assembly and activity, was decreased dramatically in the 827G cybrids.[41] Complex I is the largest complex (approximately 1000 kD) of the 5 OXPHOS complexes and occupies the initial position in the respiratory electron transport chain (I-III-IV); thus, decreased complex I levels obviously affect mitochondrial function.[42,43] Consistent with these findings, we found decreased respiration chain function and increased ROS levels along with downregulated complex I activity in the 827G cybrids compared with the 827A cybrids. These changes further activated mitochondrial-nuclear signaling pathways, including the JNK and AMPK signaling pathways. JNK signaling can downregulate RXRα transcript levels and OXPHOS complex biogenesis, which further aggravates mitochondrial OXPHOS and lipid metabolism dysfunction.[44] On the other hand, evidence has shown that lipid metabolism dysfunction induced PPARα downregulation, which may inhibit the expression of PPARα/RXR.[45,46] Moreover, AMPK activation may increase the expression of the transporter ABCG5/8 to increase the risk of cholesterol entering the bile and gallbladder.[47] As shown in Figure 6, we similarly found that the 827G cybrids showed decreased PPARα and RXRα expression, which may have inhibited cholesterol efflux into peripheral blood by downregulating the expression of the transporter ABCA1, while promoting cholesterol efflux into the bile and gallbladder by increasing the expression of transporter ABCG5/8.

As previously described, hypoxia is a risk factor for the formation of gallstones. One study has demonstrated that adipocyte HIF2α reduces atherosclerosis by promoting ceramide catabolism and thus increasing hepatic cholesterol elimination to the gallbladder.[48] Additionally, activation of the HIF1α subunit pathway in steatotic liver contributes to the formation of gallstones.[28] Consistent with previous studies, our study indicated that the levels of ABCG5/8 were dramatically higher in the 827G cybrids compared than in the 827A cybrids and that this difference was partly dependent on the HIF1α pathway. Notably, such increases in ABCG5/8 levels may increase the risk of gallstones by reinforcing activation of AMPK signaling under hypoxia.[49,50] Interestingly, in our gallstone cases, the blood lipid levels did not exceed the upper limit. These findings provide a possible explanation for why mtDNA 827A>G preferentially increases the risk of cholesterol gallstones rather than atherosclerosis.

Accumulating evidence has shown that the prevalence of gallstones among Native Americans is the highest in the world.[7,51] Interestingly, a high frequency of haplogroup B, almost all of which are haplogroup B2 (1 of the branches of haplogroup B4b), has also been observed in Native Americans.[52,53] For example, the Pima Indian, the most commonly studied Amerindian tribe in the context of gallbladder diseases, has the highest prevalence of gallstone and the highest frequency of haplogroup B2 among Native Americans.[54,55] It has also been shown that the prevalence of gallbladder diseases increases in Chilean populations with increasing level of Native Americans admixture as measured by analysis of mtDNA and other genetic markers.[56] It seems that the presence of mtDNA haplogroup B4b′d′e′j is responsible for the ethnic differences in gallstone and even

other metabolic disorders, in America. Interestingly, the frequencies of 827A>G B4 carriers in Africa, Europe, and South and West Asia were found to be generally low in the current study, but the prevalence of gallstone disease was also considerable (4%–23%) (Figure 1*C*), indicating that genetic risks other than the mtDNA variant 827A>G or environmental factors, such as lifestyles, are also important in gallstone disease. Therefore, our study, to some extent,

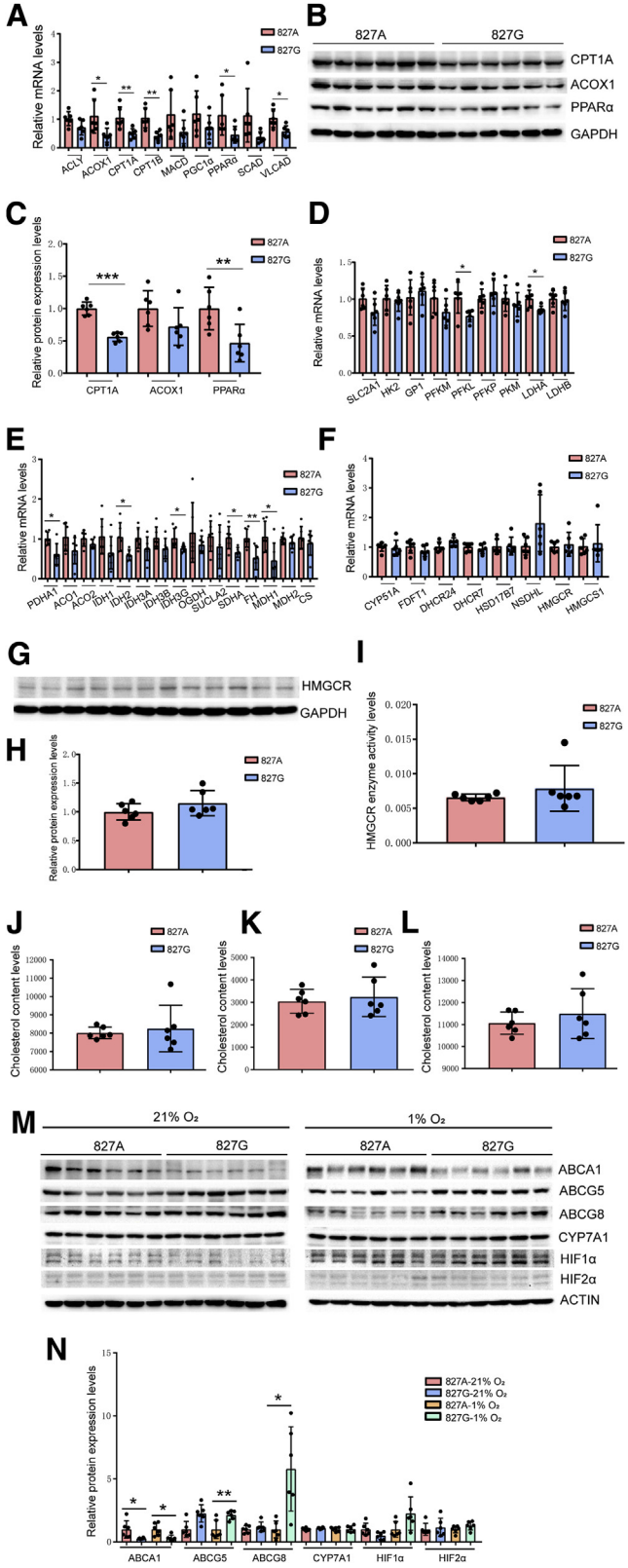

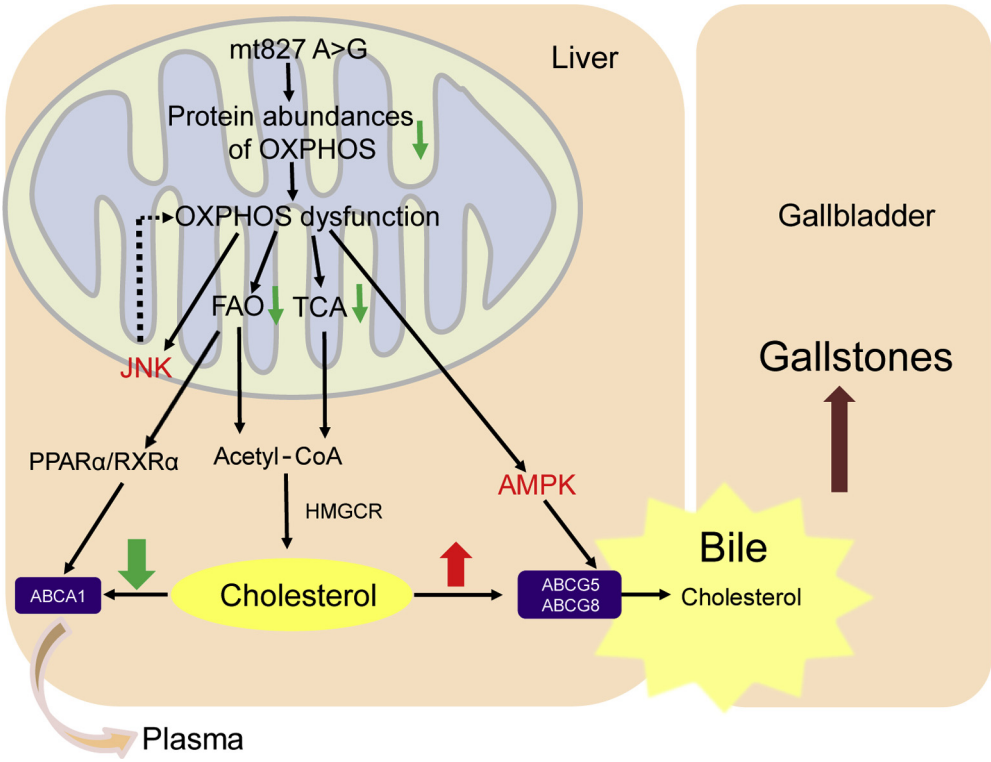

Figure 6. Schematic of the mechanism of abnormal cholesterol transport in the 827G cybrids. A possible pathologic mechanism of cholesterol gallstone formation in the 827G cybrids. The 827A>G variant of the B4b′d′e′j haplogroups led to decreased abundance of proteins related to OXPHOS and to further dysfunction. On the one hand, the levels of acetyl co-enzyme A, used for cholesterol synthesis, decreased due to downregulation of fatty acid oxidation and TCA metabolism processes; on the other hand, high ROS levels in the 827G cybrids further activated mitochondrial retrograde signaling pathways, including the JNK and AMPK pathways. The JNK pathway reduced biogenesis of OXPHOS complexes, which further aggregated mitochondrial dysfunction. Moreover, downregulation of PPARα/RXRα inhibited cholesterol efflux into peripheral blood through the transporter ABCA1. However, AMPK activation may have increased the levels of the transporter ABCG5/8, thus increasing the risk of cholesterol entering the bile and gallbladder.

Figure 5. (***See previous page***). **The lipid metabolism and cholesterol transport processes were abnormal in the 827G cybrids.** (*A*) Lipid metabolism process–associated gene expression in the 827A (n = 6) and 827G (n = 6) cybrids. Relative gene expression in the 827G cybrids was normalized to the 827A cybrids. (*B*) Immunoblotting analysis of the levels of CPT1A, ACOX1, and PPARα in whole-cell extracts from the 827A (n = 6) and 827G (n = 6) cybrids. GAPDH was used as a loading control. (*C*) Quantified signal intensities of all the target protein bands/ACTIN bands. The protein levels in the 827G cybrids were normalized to those in the 827A cybrids (the mean value for cybrids 827A was set to 1). (*D*) Glycolysis process–associated gene expression in the 827A (n = 6) and 827G (n = 6) cybrids. The relative gene expression in the 827G cybrids was normalized to the expression in the 827A cybrids. (*E*) TCA process-associated gene expression in the 827A (n = 6) and 827G (n = 6) cybrids. The relative gene expression in the 827G cybrids was normalized to the expression in the 827A cybrids. (*F*) Cholesterol synthesis process–associated gene expression in the 827A (n = 6) and 827G (n = 6) cybrids. The relative gene expression in the 827G cybrids was normalized to the expression in the 827A cybrids. (*G*) Representative Western blot of the cholesterol synthesis rate-limiting enzyme HMGCR in whole-cell extracts from the 827A (n = 6) and 827G (n = 6) cybrids. GAPDH was used as a loading control. (*H*) Quantified signal intensities of HMGCR protein bands/GAPDH bands. The levels of proteins in the 827G cybrids were normalized to those in the 827A cybrids (the mean value for 827A cybrids was set to 1). (*I*) HMGCR enzymatic activity detection in the 827A (n = 6) and 827G (n = 6) cybrids. The relative activity in the 827G cybrids was normalized to the activity in the 827A cybrids. (*J*) Whole-cell cholesterol content in the 827A (n = 6) and 827G (n = 6) cybrids. The relative content in the 827G cybrids was normalized to the content in the 827A cybrids. (*K*) Cholesterol efflux into the cultured medium of the 827A (n = 6) and 827G (n = 6) cybrids. The relative efflux for the 827G cybrids was normalized to the efflux for the 827A cybrids. (*L*) Total whole-cell and medium cholesterol content for the 827A (n = 6) and 827G (n = 6) cybrids. The relative content in the 827G cybrids was normalized to the content in the 827A cybrids. (*M*) Representative Western blot of ABCA1, ABCG5, ABCG8, CYP7A1, HIF1α, and HIF2α in whole-cell extracts from the 827A (n = 6) and 827G (n = 6) cybrids under 21% O_2, and 1% O_2, respectively. ACTIN was used as a loading control. The protein levels in the 827G cybrids were normalized to those in the 827A cybrids. (*N*) Quantified signal intensities of all the target protein bands/ACTIN bands. The levels of proteins in the 827G cybrids were normalized to those in the 827A cybrids (the mean value for cybrids 827A was set to 1). The data are presented as the mean ± SD for at least 3 independent tests per experiment. **P* < .05; ***P* < .01; ****P* < .001.

explained the etiology underlying the susceptibility to gallstone disease in Native Americans.

In summary, our study demonstrates a potential link between mtDNA 827A>G and gallstone disease. We have revealed that mtDNA 827A>G induces aberrant mitochondrial function and abnormal cholesterol transport, resulting in increased occurrence of gallstones. Our findings provide a significant biological basis for the clinical diagnosis and prevention of gallstone disease in the future.

Materials and Methods

Study Participants

Blood samples of 104 cases and 300 controls were collected in the Greater Shanghai Area with informed consent. The protocol of the study was approved by the Ethical Committee of the Chinese National Human Genome Center in Shanghai. The presence (cases) or absence (controls) of gallstone disease (cholelithiasis) was diagnosed by ultrasound and/or cholecystectomy. The mean age of onset in the patients was 44.9 (range, 19–81) years, and all controls were above 50 years of age (mean age 64.0 years; range, 50–86 years). The proportions of men among the cases and controls were 46.8% and 54.0%, respectively.

DNA samples from the blood of 206 827A (B4a/c)- and 82 827G (B4b′d′e′j)- genotype participants and all platelet samples from healthy individuals used to construct the transmitochondrial cybrids model were obtained from the Taizhou Institute of Health Sciences, Fudan University. The study was approved by the Human Ethics Committee of Fudan University.

mtDNA Sequencing, Genotyping, Median-Joining Network Analysis, Conservation Analysis, and RNA Structure Analysis

Genomic DNA from peripheral blood was extracted using a standard SDS lysis protocol for genotyping. HVS1 and other sites (8281–8289 deletion, 827A>G, 499G>A, 13942A>G, 6023G>A, and 6413T>C) in the coding region were genotyped by sequencing or polymerase chain reaction–restriction fragment length polymorphism assay. For complete sequence analysis of certain samples, Sanger sequencing was performed using 24 previously reported pairs of mtDNA primers.[57] The single nucleotide polymorphisms (SNPs) in each participant were identified by comparing the obtained sequences with the revised Cambridge Reference Sequence by using Codon Code Aligner 3.0.1 (Codon Code Corporation, Centerville, VA). The mtDNA haplogroup was assigned by comparing the target SNPs with the SNPs of the most up-to-date Chinese mtDNA haplogroup tree.[36] A median-joining phylogeny of these individuals was reconstructed using NETWORK software (Fluxus Technology Ltd, Colchester, Essex). Conservation analysis of 827 nucleotides was performed with UGENE software (NCIT UNIPRO, LLC, Novosibirsk, Russia). The RNA structure analysis of 12S rRNA with 827A or 827G was performed using the RNAfold program in the Vienna RNA Package 2.0.

Cell Line Generation and Culture Conditions

143B ρ0 human osteosarcoma cells lacking mtDNA were cultured in high-glucose Dulbecco's modified Eagle medium (Thermo Fisher Scienetific, Waltham, MA) containing 10% fetal bovine serum (Thermo Fisher Scienetific), 100-μg/mL pyruvate, and 50-μg/mL uridine. Transmitochondrial cybrids were formed by fusing 143B ρ0 cells and platelets from healthy individuals with different haplogroups, as described previously.[35] In this study, 12 cybrids distributed in an mtDNA tree were constructed, including 6 B4a/B4c-haplogroup cybrids (named 827A cybrids) and 6 B4b/B4d-haplogroup cybrids (named 827G cybrids). All plasma samples were collected from Taizhou. The cybrids were cultured in high-glucose DMEM containing 10% fetal bovine serum at 37°C in an atmosphere with 5% CO_2. Pathogenic mtDNA mutations and cross-contamination during single-clone selection were ruled out through Sanger sequencing of the whole mitochondrial genome in all cybrid cells during culture (Supplementary Table 2).

Analyses of mtDNA Content, Mitochondrial RNA, Mitochondrial Ribosome Subunits, Mitophagy, and Metabolism-Associated Gene Expression

Both mtDNA content and the mRNA levels of 13 mtDNA-encoded OXPHOS subunits were determined using the $2^{(-\Delta\Delta CT)}$ method as previously described.[58] Briefly, genomic DNA and total RNA were extracted using standard protocols, and the total RNA was then treated with DNase and reverse-transcribed using 6 random primers (Takara, Dalian, China). Quantitative real-time polymerase chain reaction was performed using primers targeted to mtDNA, mitochondrial RNA, a subset of mitochondrial ribosome subunits, mitophagy-related genes, metabolism-related genes, and nuclear housekeeping genes on a QuantStudio 7 Flex Real-Time polymerase chain reaction system (Thermo Fisher Scientific) by using SYBR Green qPCR Mastermix (Takara). All primers used in these analyses are listed in Supplementary Table 3.

Mitochondria Isolation and Respiratory Chain Complex Enzymatic Activity Assay

Mitochondria from cultured cybrids were isolated as previously described.[59] The enzymatic activity of 4 respiratory chain complexes was measured in the mitochondria of cybrids as previously described.[39] The respiratory chain complex enzymatic activity in each case was normalized against that of citrate synthase, a mitochondrial matrix marker enzyme.

Immunoblotting and Antibodies

Proteins were extracted using RIPA lysis buffer (Cell Signaling Technology, Danvers, MA) supplemented with a protease inhibitor cocktail (Sigma-Aldrich, St. Louis, MO). Thirty micrograms of protein was separated using 10% sodium dodecyl sulfate polyacrylamide gel electrophoresis and then transferred onto polyvinylidene fluoride

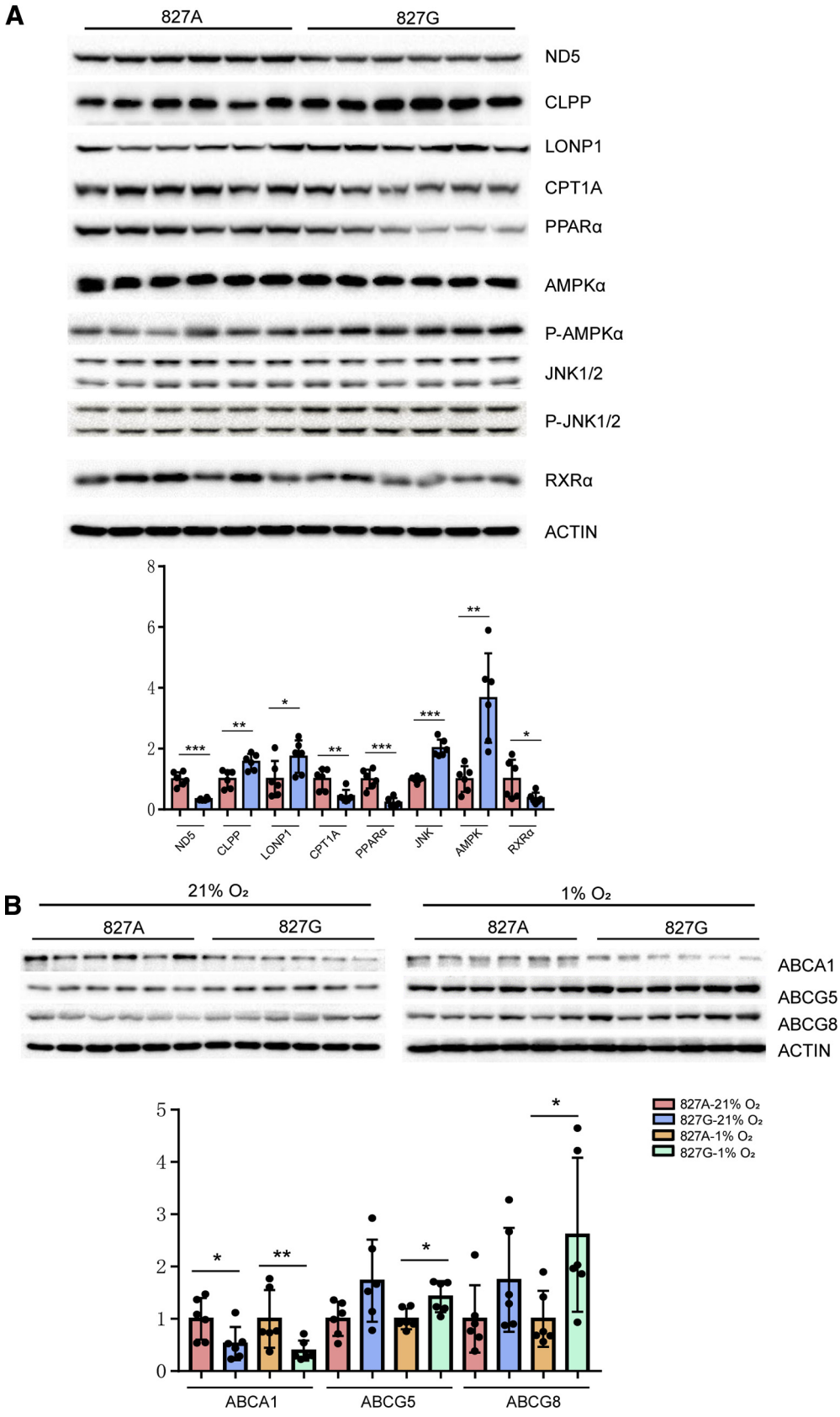

Figure 7. Immunoblotting validation analysis of the differentially expressed proteins. (*A*) Representative Western blot of proteins ND5, CLPP, LONP1, CPT1A, PPARα, AMPKα, P-AMPKα, JNK1/2, P-JNK1/2, and RXRα in whole-cell extracts from the 827A (n = 6) and 827G (n = 6) cybrids. ACTIN was used as a loading control. The protein levels in the 827G cybrids were normalized to those in the 827A cybrids. (*M*) Representative Western blot of ABCA1, ABCG5, and ABCG8 in whole-cell extracts from the 827A (n = 6) and 827G (n = 6) cybrids under 21% O_2, and 1% O_2, respectively. ACTIN was used as a loading control. The protein levels in the 827G cybrids were normalized to those in the 827A cybrids. *$P < .05$; **$P < .01$; ***$P < .001$.

membranes. The proteins were blotted with antibodies at a dilution of 1:1000, as listed in Supplementary Table 4, and detected with ECL reagents (Bio-Rad, Hercules, CA). The validation data of the differentially expressed proteins was presented in Figure 7.

ATP, ROS, Oxygen Consumption, and Cholesterol Measurements

ATP content and ROS levels were determined using an ATP measurement kit and MitoSOX (Thermo Fisher Scientific), respectively, as previously described.[57] Endogenous oxygen consumption in intact cells was determined using an Oxygraph-2k (Oroboros, Innsbruck, Austria) as described previously.[60] After recording basal respiration, oligomycin (2.5 μg/mL) (Sigma) was added to measure phosphorylation-coupled respiration. The total cellular cholesterol and free cholesterol in the cell culture medium were determined using a Total Cholesterol Quantitation Kit (Applygen, Beijing, China) and a Cholesterol Quantitation Kit (Sigma-Aldrich), respectively, according to the manufacturers' instructions.

Sample Preparation, RNA Sequencing, and Gene Expression Data Analysis

Total RNA was isolated from six 827A and six 827G cybrids using TRIzol reagent (Ambion, Austin, TX) and then purified using poly-T-attached magnetic beads (Vazyme, Nanjing, China). After fragmenting the mRNA, first-strand complementary DNA was synthesized and then sequenced using a NovaSeq 6000 platform (Illumina, San Diego, CA) as described previously. To obtain high-quality reads, reads containing adaptors, reads containing adaptor sequences, and poly-N and low-quality reads were removed from the raw data. The reference genome and gene model annotation files were downloaded directly from genome websites. The reference genome was built using STAR, and paired-end high-quality reads were aligned to the reference genome by using STAR (v2.5.1b). HTSeq v0.6.0 was used to count the reads mapped to each gene, after which the fragments per kilobase million value of each gene was calculated based on the length of the gene and the number of reads mapped to the gene. Differential expression analysis was performed using the DESeq2 R package. DESeq2 provides statistical routines for determining differential expression from digital gene expression data by using a model based on the negative binomial distribution. A heatmap of gene expression between six 827A cybrids and six 827G cybrids was created.

Statistical Analysis

The associations of mtDNA variants with gallstone disease were investigated with both the chi-square test and Fisher's exact test. The odds ratio and 95% confidence interval were calculated to evaluate the level of risk. The data are presented as the mean ± SD from 3 independent experiments. Means were compared using independent Student's t tests using SPSS 21.0 software (IBM, Armonk, NY, USA), and $P < .05$ was considered to indicate significance.

References

1. Admirand WH, Small DM. The physicochemical basis of cholesterol gallstone formation in man. J Clin Invest 1968;47:1043–1052.
2. Kosters A, Jirsa M, Groen AK. Genetic background of cholesterol gallstone disease. Biochim Biophys Acta 2003;1637:1–19.
3. Stokes CS, Krawczyk M, Lammert F. Gallstones: environment, lifestyle and genes. Dig Dis 2011;29:191–201.
4. Gilat T, Feldman C, Halpern Z, Dan M, Bar-Meir S. An increased familial frequency of gallstones. Gastroenterology 1983;84:242–246.
5. Everhart JE, Khare M, Hill M, Maurer KR. Prevalence and ethnic differences in gallbladder disease in the United States. Gastroenterology 1999;117:632–639.
6. Nakeeb A, Comuzzie AG, Martin L, Sonnenberg GE, Swartz-Basile D, Kissebah AH, Pitt HA. Gallstones: genetics versus environment. Ann Surg 2002; 235:842–849.
7. Everhart JE, Yeh F, Lee ET, Hill MC, Fabsitz R, Howard BV, Welty TK. Prevalence of gallbladder disease in American Indian populations: findings from the Strong Heart Study. Hepatology 2002;35:1507–1512.
8. Buch S, Schafmayer C, Volzke H, Becker C, Franke A, von Eller-Eberstein H, Kluck C, Bassmann I, Brosch M, Lammert F, Miquel JF, Nervi F, Wittig M, Rosskopf D, Timm B, Holl C, Seeger M, ElSharawy A, Lu T, Egberts J, Fandrich F, Folsch UR, Krawczak M, Schreiber S, Nurnberg P, Tepel J, Hampe J. A genome-wide association scan identifies the hepatic cholesterol transporter ABCG8 as a susceptibility factor for human gallstone disease. Nat Genet 2007;39:995–999.
9. Buch S, Schafmayer C, Volzke H, Seeger M, Miquel JF, Sookoian SC, Egberts JH, Arlt A, Pirola CJ, Lerch MM, John U, Franke A, von Kampen O, Brosch M, Nothnagel M, Kratzer W, Boehm BO, Broring DC, Schreiber S, Krawczak M, Hampe J. Loci from a genome-wide analysis of bilirubin levels are associated with gallstone risk and composition. Gastroenterology 2010;139:1942–1951.e2.
10. Di MA. Therapy of digestive disorders: A companion to sleisenger and Fordtran's gastrointestinal and liver disease. Gastroenterology 2000;118:1275–1276.
11. Biddinger SB, Haas JT, Yu BB, Bezy O, Jing E, Zhang W, Unterman TG, Carey MC, Kahn CR. Hepatic insulin resistance directly promotes formation of cholesterol gallstones. Nat Med 2008;14:778–782.
12. Uppal H, Zhai Y, Gangopadhyay A, Khadem S, Ren S, Moser JA, Xie W. Activation of liver X receptor sensitizes mice to gallbladder cholesterol crystallization. Hepatology 2008;47:1331–1342.
13. Garcia-Berumen CI, Ortiz-Avila O, Vargas-Vargas MA, Del Rosario-Tamayo BA, Guajardo-Lopez C, Saavedra-Molina A, Rodriguez-Orozco AR, Cortes-Rojo C. The severity of rat liver injury by fructose and high fat depends on the degree of respiratory dysfunction and oxidative stress induced in mitochondria. Lipids Health Dis 2019;18:78.
14. Mahmood S, Birkaya B, Rideout TC, Patel MS. Lack of mitochondria-generated acetyl-CoA by pyruvate

dehydrogenase complex downregulates gene expression in the hepatic de novo lipogenic pathway. Am J Physiol Endocrinol Metab 2016;311:E117–E127.
15. Chen J, Hattori Y, Nakajima K, Eizawa T, Ehara T, Koyama M, Hirai T, Fukuda Y, Kinoshita M, Sugiyama A, Hayashi J, Onaya T, Kobayashi T, Tawata M. Mitochondrial complex I activity is significantly decreased in a patient with maternally inherited type 2 diabetes mellitus and hypertrophic cardiomyopathy associated with mitochondrial DNA C3310T mutation: a cybrid study. Diabetes Res Clin Pract 2006;74:148–153.
16. Liao WQ, Pang Y, Yu CA, Wen JY, Zhang YG, Li XH. Novel mutations of mitochondrial DNA associated with type 2 diabetes in Chinese Han population. Tohoku J Exp Med 2008;215:377–384.
17. Wang S, Wu S, Zheng T, Yang Z, Ma X, Jia W, Xiang K. Mitochondrial DNA mutations in diabetes mellitus patients in Chinese Han population. Gene 2013;531:472–475.
18. Wilson FH, Hariri A, Farhi A, Zhao H, Petersen KF, Toka HR, Nelson-Williams C, Raja KM, Kashgarian M, Shulman GI, Scheinman SJ, Lifton RP. A cluster of metabolic defects caused by mutation in a mitochondrial tRNA. Science 2004;306:1190–1194.
19. Wang S, Li R, Fettermann A, Li Z, Qian Y, Liu Y, Wang X, Zhou A, Mo JQ, Yang L, Jiang P, Taschner A, Rossmanith W, Guan MX. Maternally inherited essential hypertension is associated with the novel 4263A>G mutation in the mitochondrial tRNAIle gene in a large Han Chinese family. Circ Res 2011;108:862–870.
20. Kokaze A, Ishikawa M, Matsunaga N, Karita K, Yoshida M, Shimada N, Ohtsu T, Shirasawa T, Ochiai H, Satoh M, Hashimoto M, Hoshino H, Takashima Y. Mitochondrial DNA 5178 C/A polymorphism influences the effects of habitual smoking on the risk of dyslipidemia in middle-aged Japanese men. Lipids Health Dis 2012;11:97.
21. Hroudova J, Fisar Z. Control mechanisms in mitochondrial oxidative phosphorylation. Neural Regen Res 2013;8:363–375.
22. Qin J, Han TQ, Fei J, Jiang ZY, Zhang Y, Yang SY, Jiang ZH, Cai XX, Huang W, Zhang SD. Risk factors of familial gallstone disease: study of 135 pedigrees. Zhonghua Yi Xue Za Zhi 2005;85:1966–1969.
23. Zheng HX, Yan S, Qin ZD, Wang Y, Tan JZ, Li H, Jin L. Major population expansion of East Asians began before neolithic time: evidence of mtDNA genomes. PLoS One 2011;6:e25835.
24. Behar DM, van Oven M, Rosset S, Metspalu M, Loogvali EL, Silva NM, Kivisild T, Torroni A, Villems R. A "Copernican" reassessment of the human mitochondrial DNA tree from its root. Am J Hum Genet 2012;90:675–684.
25. Fagundes NJ, Kanitz R, Eckert R, Valls AC, Bogo MR, Salzano FM, Smith DG, Silva WA Jr, Zago MA, Ribeiro-dos-Santos AK, Santos SE, Petzl-Erler ML, Bonatto SL. Mitochondrial population genomics supports a single pre-Clovis origin with a coastal route for the peopling of the Americas. Am J Hum Genet 2008;82:583–592.
26. Zheng HX, Yan S, Qin ZD, Jin L. MtDNA analysis of global populations support that major population expansions began before Neolithic Time. Sci Rep 2012;2:745.
27. Lorenz R, Bernhart SH, Honer Zu Siederdissen C, Tafer H, Flamm C, Stadler PF, Hofacker IL. ViennaRNA package 2.0. Algorithms Mol Biol 2011;6:26.
28. Asai Y, Yamada T, Tsukita S, Takahashi K, Maekawa M, Honma M, Ikeda M, Murakami K, Munakata Y, Shirai Y, Kodama S, Sugisawa T, Chiba Y, Kondo Y, Kaneko K, Uno K, Sawada S, Imai J, Nakamura Y, Yamaguchi H, Tanaka K, Sasano H, Mano N, Ueno Y, Shimosegawa T, Katagiri H. Activation of the hypoxia inducible factor 1alpha subunit pathway in steatotic liver contributes to formation of cholesterol gallstones. Gastroenterology 2017;152:1521–1535.e8.
29. Sharma MR, Koc EC, Datta PP, Booth TM, Spremulli LL, Agrawal RK. Structure of the mammalian mitochondrial ribosome reveals an expanded functional role for its component proteins. Cell 2003;115:97–108.
30. Gopisetty G, Thangarajan R. Mammalian mitochondrial ribosomal small subunit (MRPS) genes: A putative role in human disease. Gene 2016;589:27–35.
31. Ozawa T, Katsumata K, Hayakawa M, Tanaka M, Sugiyama S, Tanaka T, Itoyama S, Nunoda S, Sekiguchi M. Genotype and phenotype of severe mitochondrial cardiomyopathy: a recipient of heart transplantation and the genetic control. Biochem Biophys Res Commun 1995;207:613–620.
32. Xing G, Chen Z, Wei Q, Tian H, Li X, Zhou A, Bu X, Cao X. Maternally inherited non-syndromic hearing loss associated with mitochondrial 12S rRNA A827G mutation in a Chinese family. Biochem Biophys Res Commun 2006;344:1253–1257.
33. Rydzanicz M, Wrobel M, Pollak A, Gawecki W, Brauze D, Kostrzewska-Poczekaj M, Wojsyk-Banaszak I, Lechowicz U, Mueller-Malesinska M, Oldak M, Ploski R, Skarzynski H, Szyfter K. Mutation analysis of mitochondrial 12S rRNA gene in Polish patients with non-syndromic and aminoglycoside-induced hearing loss. Biochem Biophys Res Commun 2010;395:116–121.
34. Zhu Y, Zhao J, Feng B, Su Y, Kang D, Yuan H, Zhai S, Dai P. Mutations in the mitochondrial 12S rRNA gene in elderly Chinese people. Acta Otolaryngol 2015;135:26–34.
35. King MP, Attardi G. Human cells lacking mtDNA: repopulation with exogenous mitochondria by complementation. Science 1989;246:500–503.
36. Zhou H, Nie K, Qiu R, Xiong J, Shao X, Wang B, Shen L, Lyu J, Fang H. Generation and bioenergetic profiles of cybrids with East Asian mtDNA haplogroups. Oxid Med Cell Longev 2017;2017:1062314.
37. Ji F, Sharpley MS, Derbeneva O, Alves LS, Qian P, Wang Y, Chalkia D, Lvova M, Xu J, Yao W, Simon M, Platt J, Xu S, Angelin A, Davila A, Huang T, Wang PH, Chuang LM, Moore LG, Qian G, Wallace DC. Mitochondrial DNA variant associated with Leber hereditary optic neuropathy and high-altitude Tibetans. Proc Natl Acad Sci U S A 2012;109:7391–71396.
38. Fang H, Hu N, Zhao Q, Wang B, Zhou H, Fu Q, Shen L, Chen X, Shen F, Lyu J. mtDNA haplogroup N9a increases the risk of type 2 diabetes by altering mitochondrial function and intracellular mitochondrial signals. Diabetes 2018;67:1441–1453.

39. Fang H, Zhang F, Li F, Shi H, Ma L, Du M, You Y, Qiu R, Nie H, Shen L, Bai Y, Lyu J. Mitochondrial DNA haplogroups modify the risk of osteoarthritis by altering mitochondrial function and intracellular mitochondrial signals. Biochim Biophys Acta 2016;1862:829–836.
40. Hua S, Li M, Zhao Q, Wang J, Zhou Y, Liu J, Fang H, Jiang M, Shen L. Mitochondrial DNA haplogroup N9a negatively correlates with incidence of hepatocellular carcinoma in Northern China. Mol Ther Nucleic Acids 2019;18:332–340.
41. Bourges I, Ramus C, Mousson de Camaret B, Beugnot R, Remacle C, Cardol P, Hofhaus G, Issartel JP. Structural organization of mitochondrial human complex I: role of the ND4 and ND5 mitochondria-encoded subunits and interaction with prohibitin. Biochem J 2004;383:491–499.
42. Alston CL, Morak M, Reid C, Hargreaves IP, Pope SA, Land JM, Heales SJ, Horvath R, Mundy H, Taylor RW. A novel mitochondrial MTND5 frameshift mutation causing isolated complex I deficiency, renal failure and myopathy. Neuromuscul Disord 2010;20:131–135.
43. Zhang J, Ji Y, Lu Y, Fu R, Xu M, Liu X, Guan MX. Leber's hereditary optic neuropathy (LHON)-associated ND5 12338T > C mutation altered the assembly and function of complex I, apoptosis and mitophagy. Hum Mol Genet 2018;27:1999–2011.
44. Chae S, Ahn BY, Byun K, Cho YM, Yu MH, Lee B, Hwang D, Park KS. A systems approach for decoding mitochondrial retrograde signaling pathways. Sci Signal 2013;6:rs4.
45. Dushkin MI, Khoshchenko OM, Posokhova EN, Schvarts Y. Agonists of PPAR-alpha, PPAR-gamma, and RXR inhibit the formation of foam cells from macrophages in mice with inflammation. Bull Exp Biol Med 2007;144:713–716.
46. Agassandian M, Miakotina OL, Andrews M, Mathur SN, Mallampalli RK. Pseudomonas aeruginosa and sPLA2 IB stimulate ABCA1-mediated phospholipid efflux via ERK-activation of PPARalpha-RXR. Biochem J 2007; 403:409–420.
47. Molusky MM, Hsieh J, Lee SX, Ramakrishnan R, Tascau L, Haeusler RA, Accili D, Tall AR. Metformin and AMP kinase activation increase expression of the sterol transporters ABCG5/8 (ATP-binding cassette transporter G5/G8) with potential antiatherogenic consequences. Arterioscler Thromb Vasc Biol 2018;38:1493–1503.
48. Zhang X, Zhang Y, Wang P, Zhang SY, Dong Y, Zeng G, Yan Y, Sun L, Wu Q, Liu H, Liu B, Kong W, Wang X, Jiang C. Adipocyte hypoxia-inducible factor 2alpha suppresses atherosclerosis by promoting adipose ceramide catabolism. Cell Metab 2019;30:937–951.e5.
49. Dengler F. Activation of AMPK under hypoxia: many roads leading to Rome. Int J Mol Sci 2020;21:2428.
50. Mungai PT, Waypa GB, Jairaman A, Prakriya M, Dokic D, Ball MK, Schumacker PT. Hypoxia triggers AMPK activation through reactive oxygen species-mediated activation of calcium release-activated calcium channels. Mol Cell Biol 2011;31:3531–3545.
51. Carey MC, Paigen B. Epidemiology of the American Indians' burden and its likely genetic origins. Hepatology 2002;36:781–791.
52. Silva WA Jr, Bonatto SL, Holanda AJ, Ribeiro-Dos-Santos AK, Paixao BM, Goldman GH, Abe-Sandes K, Rodriguez-Delfin L, Barbosa M, Paco-Larson ML, Petzl-Erler ML, Valente V, Santos SE, Zago MA. Mitochondrial genome diversity of Native Americans supports a single early entry of founder populations into America. Am J Hum Genet 2002;71:187–192.
53. Tamm E, Kivisild T, Reidla M, Metspalu M, Smith DG, Mulligan CJ, Bravi CM, Rickards O, Martinez-Labarga C, Khusnutdinova EK, Fedorova SA, Golubenko MV, Stepanov VA, Gubina MA, Zhadanov SI, Ossipova LP, Damba L, Voevoda MI, Dipierri JE, Villems R, Malhi RS. Beringian standstill and spread of Native American founders. PLoS One 2007;2:e829.
54. Wallace DC, Torroni A. American Indian prehistory as written in the mitochondrial DNA: a review. Hum Biol 1992;64:403–416.
55. Grimaldi CH, Nelson RG, Pettitt DJ, Sampliner RE, Bennett PH, Knowler WC. Increased mortality with gallstone disease: results of a 20-year population-based survey in Pima Indians. Ann Intern Med 1993;118:185–190.
56. Miquel JF, Covarrubias C, Villaroel L, Mingrone G, Greco AV, Puglielli L, Carvallo P, Marshall G, Del Pino G, Nervi F. Genetic epidemiology of cholesterol cholelithiasis among Chilean Hispanics, Amerindians, and Maoris. Gastroenterology 1998;115:937–946.
57. Fang H, Shi H, Li X, Sun D, Li F, Li B, Ding Y, Ma Y, Liu Y, Zhang Y, Shen L, Bai Y, Yang Y, Lu J. Exercise intolerance and developmental delay associated with a novel mitochondrial ND5 mutation. Sci Rep 2015;5:10480.
58. Sun D, Li B, Qiu R, Fang H, Lyu J. Cell type-specific modulation of respiratory chain supercomplex organization. Int J Mol Sci 2016;17:926.
59. Claude A, Fullam EF. An electron microscope study of isolated mitochondria: method and preliminary results. J Exp Med 1945;81:51–62.
60. Xu B, Li X, Du M, Zhou C, Fang H, Lyu J, Yang Y. Novel mutation of ND4 gene identified by targeted next-generation sequencing in patient with Leigh syndrome. J Hum Genet 2017;62:291–297.

Received August 19, 2020. Accepted November 30, 2020.

Correspondence
Address correspondence to: Li Jin, PhD, School of Life Sciences, Fudan University, 2005 Songhu Road, Shanghai, China. e-mail: lijin@fudan.edu.cn; fax: 862131246607; OR Jiucun Wang, PhD, School of Life Sciences, Fudan University, 2005 Songhu Road, Shanghai, China. e-mail: jcwang@fudan.edu.cn; fax: 862131246607.

Acknowledgments
The authors acknowledge all the participants involved in this study and the Taizhou Institute of Health Sciences, Fudan University.

Conflicts of Interest
The authors disclose no conflicts.

Funding
This work was supported by grants from the National Natural Science Foundation of China (31871436, 31521003, 91731000, 31401062), the CAMS Innovation Fund for Medical Sciences (2019-I2M-5-066), the Shanghai Municipal Science and Technology Major Project (2017SHZDZX01), the Scientific and Technology Committee of Shanghai Municipality (18490750300), and the 111 Project (B13016).

Supplementary Table 1. The Frequency of Mitochondrial Haplogroup B4b′d′e′j and the Prevalence of Gallstone Disease in Global Populations

Population	B4b′d′e′j Haplogroups (%)	Gallstone Disease (%)	References
Mapuche Indians, Chile	36.84	35.2	1,2
Peru	43.88	14.3	3,4
Argentinian	10.35	20.5	5,6
Mexican American	13.54	17.8	7,8
Puerto Rican	6.54	9.5	9,10
Mexican	26.45	14.1	11,12
Taiwan, China	3.19	6.26	13–16
Sichuan, China	2.93	10.7	16,17
Shanghai, China	4.18	5.84	16,18,19
Zhejiang, China	2.98	8.8	16,20
Jiangsu, China	4.24	4.21	16,21
Xinjiang, China	7.79	11.64	16,22
Japan	3.15	3.2	10,23
Korea	3.45	4.85	24,25
Thailand	2.11	3.1	26–28
Italy	0	13.9	10,29
British	0	23.6	10,30
Ghana	0	5.9	31,32
Tunisia	0	4	32,33
Sudan	0	5.2	27,32
India	0	6.12	10,34
Iran	0	4.7	35,36
Germany	0	21.2	37,38

Supplementary Table 2. Analysis of Whole Mitochondrial Genome of the 12 Cybrids

Position	Gene	rCRS Base	Mutation	AA Change	mtDNA Database[a]
Analysis of whole mitochondrial genome-1-B4a4					
73	D-loop	A	G	no	polymorphic site
152	D-loop	T	C	no	polymorphic site
193	D-loop	A	G	no	polymorphic site
263	D-loop	A	G	no	polymorphic site
373	D-loop	A	G	no	polymorphic site
709	12S rRNA	G	A	no	polymorphic site
750	12S rRNA	A	G	no	polymorphic site
1438	12S rRNA	A	G	no	polymorphic site
2010	16S rRNA	T	C	no	polymorphic site
2706	16S rRNA	A	G	no	polymorphic site
4769	16S rRNA	A	G	no	polymorphic site
5201	ND2	T	C	no	polymorphic site
5465	ND2	T	C	no	polymorphic site
7028	COI	C	T	no	polymorphic site
8860	ATPase6	A	G	Thr > Ala	polymorphic site
9123	ATPase6	G	A	no	polymorphic site
10289	ND3	A	G	no	polymorphic site
11719	ND4	G	A	no	polymorphic site
13269	ND5	A	G	no	polymorphic site
14751	Cytb	C	T	Thr > Ile	polymorphic site
14766	Cytb	C	T	Thr > Ile	polymorphic site
15326	Cytb	A	G	Thr > Ala	polymorphic site
16182	D-loop	A	C	no	polymorphic site
16183	D-loop	A	C	no	polymorphic site
16189	D-loop	T	C	no	polymorphic site
16217	D-loop	T	C	no	polymorphic site
16261	D-loop	C	T	no	polymorphic site
16299	D-loop	A	G	no	polymorphic site
16519	D-loop	T	C	no	polymorphic site
Analysis of whole mitochondrial genome-2-B4a1c2					
73	D-loop	A	G	no	polymorphic site
146	D-loop	T	C	no	polymorphic site
263	D-loop	A	G	no	polymorphic site
709	12S rRNA	G	A	no	polymorphic site
750	12S rRNA	A	G	no	polymorphic site
1438	12S rRNA	A	G	no	polymorphic site
2706	16S rRNA	A	G	no	polymorphic site
4769	ND2	A	G	no	polymorphic site
5465	ND2	T	C	no	polymorphic site
6080	CO1	A	T	no	polymorphic site
7028	CO1	C	T	no	polymorphic site
7052	CO1	A	G	no	polymorphic site
7271	CO1	A	G	no	polymorphic site
8860	ATPase6	A	G	Thr > Ala	polymorphic site
9123	ATPase6	G	A	no	polymorphic site
9822	CO3	C	A	Leu > Ile	polymorphic site
10238	ND3	T	C	no	polymorphic site
11719	ND4	G	A	no	polymorphic site
14766	Cytb	C	T	Thr > Ile	polymorphic site

Supplementary Table 2. Continued

Position	Gene	rCRS Base	Mutation	AA Change	mtDNA Database[a]
15326	Cytb	A	G	Thr > Ala	polymorphic site
15661	Cytb	C	T	no	polymorphic site
16167	D-loop	C	T	no	polymorphic site
16182	D-loop	A	C	no	polymorphic site
16183	D-loop	A	C	no	polymorphic site
16189	D-loop	T	C	no	polymorphic site
16217	D-loop	T	C	no	polymorphic site
16261	D-loop	C	T	no	polymorphic site
16317	D-loop	A	T	no	polymorphic site
16519	D-loop	T	C	no	polymorphic site
Analysis of whole mitochondrial genome-3-B4a					
73	D-loop	A	G	no	polymorphic site
263	D-loop	A	G	no	polymorphic site
310	D-loop	T	C	no	polymorphic site
316	D-loop	G	C	no	polymorphic site
750	12S rRNA	A	G	no	polymorphic site
1438	12S rRNA	A	G	no	polymorphic site
2706	16S rRNA	A	G	no	polymorphic site
4769	ND2	A	G	no	polymorphic site
5465	ND2	T	C	no	polymorphic site
6386	CO1	C	T	no	polymorphic site
7028	CO1	C	T	no	polymorphic site
8860	ATPase6	A	G	Thr > Ala	polymorphic site
9123	ATPase6	G	A	no	polymorphic site
11227	ND4	C	T	no	polymorphic site
11719	ND4	G	A	no	polymorphic site
13781	ND5	T	C	Ile >Thr	polymorphic site
14053	ND5	A	G	Thr > Ala	polymorphic site
14766	Cytb	C	T	Thr > Ile	polymorphic site
15326	Cytb	A	G	Thr > Ala	polymorphic site
16182	D-loop	A	C	no	polymorphic site
16183	D-loop	A	C	no	polymorphic site
16189	D-loop	T	C	no	polymorphic site
16217	D-loop	T	C	no	polymorphic site
16261	D-loop	C	T	no	polymorphic site
16299	D-loop	A	G	no	polymorphic site
16355	D-loop	C	T	no	polymorphic site
16390	D-loop	G	A	no	polymorphic site
16519	D-loop	T	C	no	polymorphic site
Analysis of whole mitochondrial genome-4-B4b1a3					
73	D-loop	A	G	no	polymorphic site
207	D-loop	G	A	no	polymorphic site
263	D-loop	A	G	no	polymorphic site
408	D-loop	T	A	no	polymorphic site
499	D-loop	G	A	no	polymorphic site
750	12S rRNA	A	G	no	polymorphic site
827	12S rRNA	A	G	no	polymorphic site
1438	12S rRNA	A	G	no	polymorphic site
2706	16S rRNA	A	G	no	polymorphic site
4769	ND2	A	G	no	polymorphic site

Supplementary Table 2. Continued

Position	Gene	rCRS Base	Mutation	AA Change	mtDNA Database[a]
4820	ND2	G	A	no	polymorphic site
6023	COI	G	A	no	polymorphic site
6413	COI	T	C	no	polymorphic site
7028	COI	C	T	no	polymorphic site
8466	ATPase8	A	G	His > Arg	polymorphic site
8860	ATPase6	A	G	Thr > Ala	polymorphic site
9055	ATPase6	G	A	Ala > Thr	polymorphic site
9338	COIII	A	T	no	polymorphic site
9615	COIII	T	C	no	polymorphic site
9966	COIII	G	A	Val > Ile	polymorphic site
11719	ND4	G	A	no	polymorphic site
13590	ND5	G	A	no	polymorphic site
14766	Cytb	C	T	Thr > Ile	polymorphic site
15326	Cytb	A	G	Thr > Ala	polymorphic site
15535	Cytb	C	T	no	polymorphic site
16136	D-loop	T	C	no	polymorphic site
16183	D-loop	A	C	no	polymorphic site
16189	D-loop	T	C	no	polymorphic site
16519	D-loop	T	C	no	polymorphic site
Analysis of whole mitochondrial genome-5-B4b1c1					
73	D-loop	A	G	no	polymorphic site
263	D-loop	A	G	no	polymorphic site
499	D-loop	G	A	no	polymorphic site
750	12S rRNA	A	G	no	polymorphic site
827	12S rRNA	A	G	no	polymorphic site
1438	12S rRNA	A	G	no	polymorphic site
1717	16S rRNA	T	C	no	polymorphic site
2706	16S rRNA	A	G	no	polymorphic site
3918	ND1	G	A	no	polymorphic site
4769	ND2	A	G	no	polymorphic site
4820	ND2	G	A	no	polymorphic site
7028	COI	C	T	no	polymorphic site
7521	tRNA Asp	G	A	no	polymorphic site
8860	ATPase6	A	G	Thr > Ala	polymorphic site
9101	ATPase6	T	G	Ile > Thr	polymorphic site
9861	COIII	T	C	Phe > Leu	polymorphic site
11239	ND4	A	G	no	polymorphic site
11719	ND4	G	A	no	polymorphic site
11914	ND4	G	A	no	polymorphic site
13590	ND5	G	A	no	polymorphic site
14587	ND6	A	G	no	polymorphic site
14766	Cytb	C	T	Thr > Ile	polymorphic site
15326	Cytb	A	G	Thr > Ala	polymorphic site
15535	Cytb	C	T	no	polymorphic site
16136	D-loop	T	C	no	polymorphic site
16183	D-loop	A	C	no	polymorphic site
16189	D-loop	T	C	no	polymorphic site
16217	D-loop	T	C	no	polymorphic site
16218	D-loop	C	T	no	polymorphic site
16519	D-loop	T	C	no	polymorphic site

Supplementary Table 2. Continued

Position	Gene	rCRS Base	Mutation	AA Change	mtDNA Database[a]
Analysis of whole mitochondrial genome-6-B4b1c					
73	D-loop	A	G	no	polymorphic site
263	D-loop	A	G	no	polymorphic site
309	D-loop	C	T	no	polymorphic site
310	D-loop	T	C	no	polymorphic site
499	D-loop	G	A	no	polymorphic site
750	12S rRNA	A	G	no	polymorphic site
827	12S rRNA	A	G	no	polymorphic site
1438	12S rRNA	A	G	no	polymorphic site
2706	16S rRNA	A	G	no	polymorphic site
4769	ND2	A	G	no	polymorphic site
4820	ND2	G	A	no	polymorphic site
7028	COI	C	T	no	polymorphic site
7080	COI	T	C	Phe > Leu	polymorphic site
8343	tRNA Lys	A	G	no	polymorphic site
8860	ATPase6	A	G	Thr > Ala	polymorphic site
11719	ND4	G	A	no	polymorphic site
13401	ND5	T	C	no	polymorphic site
13590	ND5	G	A	no	polymorphic site
14587	ND6	A	G	no	polymorphic site
14766	Cytb	C	T	Thr > Ile	polymorphic site
15535	Cytb	C	T	no	polymorphic site
16136	D-loop	T	C	no	polymorphic site
16182	D-loop	A	C	no	polymorphic site
16183	D-loop	A	C	no	polymorphic site
16189	D-loop	T	C	no	polymorphic site
16217	D-loop	T	C	no	polymorphic site
16218	D-loop	C	T	no	polymorphic site
16519	D-loop	T	C	no	polymorphic site
Analysis of whole mitochondrial genome-7-B4c1b2c					
73	D-loop	A	G	no	polymorphic site
150	D-loop	C	A	no	polymorphic site
263	D-loop	A	G	no	polymorphic site
709	12S rRNA	G	A	no	polymorphic site
750	12S rRNA	A	G	no	polymorphic site
1119	12S rRNA	T	C	no	polymorphic site
1438	12S rRNA	A	G	no	polymorphic site
2706	16S rRNA	A	G	no	polymorphic site
3394	ND1	T	C	Tyr > His	polymorphic site
3435	ND1	C	T	no	polymorphic site
3497	ND1	C	T	Ala > Val	polymorphic site
3571	ND1	C	T	Leu > Phe	polymorphic site
4173	ND1	A	G	no	polymorphic site
4769	ND2	A	G	no	polymorphic site
7028	COI	C	T	no	polymorphic site
8860	ATPase6	A	G	Thr > Ala	polymorphic site
9123	ATPase6	G	A	no	polymorphic site
11440	ND4	G	A	no	polymorphic site
11719	ND4	G	A	no	polymorphic site
14766	Cytb	C	T	Thr > Ile	polymorphic site

Supplementary Table 2. Continued

Position	Gene	rCRS Base	Mutation	AA Change	mtDNA Database[a]
15326	Cytb	A	G	Thr > Ala	polymorphic site
15346	Cytb	G	A	no	polymorphic site
16129	D-loop	G	A	no	polymorphic site
16140	D-loop	T	C	no	polymorphic site
16166	D-loop	A	G	no	polymorphic site
16183	D-loop	A	C	no	polymorphic site
16189	D-loop	T	C	no	polymorphic site
16217	D-loop	T	C	no	polymorphic site
16274	D-loop	G	A	no	polymorphic site
16335	D-loop	A	G	no	polymorphic site
16519	D-loop	T	C	no	polymorphic site
Analysis of whole mitochondrial genome-8-B4c1b2					
73	D-loop	A	G	no	polymorphic site
150	D-loop	C	A	no	polymorphic site
195	D-loop	T	C	no	polymorphic site
263	D-loop	A	G	no	polymorphic site
709	12S rRNA	G	A	no	polymorphic site
750	12S rRNA	A	G	no	polymorphic site
1119	12S rRNA	T	C	no	polymorphic site
1438	12S rRNA	A	G	no	polymorphic site
2706	16S rRNA	A	G	no	polymorphic site
3434	ND1	A	G	Tyr > Cys	polymorphic site
3497	ND1	C	T	Ala > Val	polymorphic site
3571	ND1	C	T	Leu > Phe	polymorphic site
4769	ND2	A	G	no	polymorphic site
7028	COI	C	T	no	polymorphic site
7175	COI	T	C	no	polymorphic site
7888	COII	C	T	no	polymorphic site
8200	COII	T	C	no	polymorphic site
8860	ATPase6	A	G	Thr > Ala	polymorphic site
10325	COIII	G	A	no	polymorphic site
11719	ND4	G	A	no	polymorphic site
13928	ND5	G	C	Ser >Thr	polymorphic site
14766	Cytb	C	T	Thr > Ile	polymorphic site
15326	Cytb	A	G	Thr > Ala	polymorphic site
15346	Cytb	G	A	no	polymorphic site
16140	D-loop	T	C	no	polymorphic site
16182	D-loop	A	C	no	polymorphic site
16183	D-loop	A	C	no	polymorphic site
16189	D-loop	T	C	no	polymorphic site
16217	D-loop	T	C	no	polymorphic site
16223	D-loop	C	T	no	polymorphic site
16274	D-loop	G	A	no	polymorphic site
16305	D-loop	A	T	no	polymorphic site
16519	D-loop	T	C	no	polymorphic site
Analysis of whole mitochondrial genome-9-B4c1b2c					
73	D-loop	A	G	no	polymorphic site
150	D-loop	C	A	no	polymorphic site
263	D-loop	A	G	no	polymorphic site
709	12S rRNA	G	A	no	polymorphic site
750	12S rRNA	A	G	no	polymorphic site

Supplementary Table 2. Continued

Position	Gene	rCRS Base	Mutation	AA Change	mtDNA Database[a]
1119	12S rRNA	T	C	no	polymorphic site
1438	12S rRNA	A	G	no	polymorphic site
1534	12S rRNA	C	T	no	polymorphic site
2706	16S rRNA	A	G	no	polymorphic site
3435	ND1	C	T	no	polymorphic site
3497	ND1	C	T	Ala > Val	polymorphic site
3571	ND1	C	T	Leu > Phe	polymorphic site
4769	ND2	A	G	no	polymorphic site
7028	COI	C	T	no	polymorphic site
8860	ATPase6	A	G	Thr > Ala	polymorphic site
9128	ATPase6	T	C	Ile > Thr	polymorphic site
9575	COIII	G	A	no	polymorphic site
10493	ND4L	T	C	no	polymorphic site
11440	ND4	G	A	no	polymorphic site
11719	ND4	G	A	no	polymorphic site
12026	ND4	A	G	Ile > Val	polymorphic site
14766	Cytb	C	T	Thr > Ile	polymorphic site
15326	Cytb	A	G	Thr > Ala	polymorphic site
15346	Cytb	G	A	no	polymorphic site
16136	D-loop	T	C	no	polymorphic site
16140	D-loop	T	C	no	polymorphic site
16183	D-loop	A	C	no	polymorphic site
16189	D-loop	T	C	no	polymorphic site
16217	D-loop	T	C	no	polymorphic site
16249	D-loop	T	C	no	polymorphic site
16274	D-loop	G	A	no	polymorphic site
16291	D-loop	C	T	no	polymorphic site
16335	D-loop	A	G	no	polymorphic site
16519	D-loop	T	C	no	polymorphic site
Analysis of whole mitochondrial genome-10-B4d1a					
73	D-loop	A	G	no	polymorphic site
263	D-loop	A	G	no	polymorphic site
272	D-loop	A	G	no	polymorphic site
750	12S rRNA	A	G	no	polymorphic site
827	12S rRNA	A	G	no	polymorphic site
1438	12S rRNA	A	G	no	polymorphic site
2706	16S rRNA	A	G	no	polymorphic site
4769	ND2	A	G	no	polymorphic site
7028	COI	C	T	no	polymorphic site
8860	ATPase6	A	G	Thr > Ala	polymorphic site
11719	ND4	G	A	no	polymorphic site
11914	ND4	G	A	no	polymorphic site
12612	ND5	A	G	no	polymorphic site
12732	ND5	T	C	no	polymorphic site
13942	ND5	A	G	Thr > Ala	polymorphic site
14034	ND5	T	C	no	polymorphic site
14766	Cytb	C	T	Thr > Ile	polymorphic site
15038	Cytb	A	G	Ile > Val	polymorphic site
15326	Cytb	A	G	Thr > Ala	polymorphic site
15535	Cytb	C	T	no	polymorphic site

Supplementary Table 2. Continued

Position	Gene	rCRS Base	Mutation	AA Change	mtDNA Database[a]
15930	tRNA Thr	G	A	no	polymorphic site
16182	D-loop	A	C	no	polymorphic site
16183	D-loop	A	C	no	polymorphic site
16189	D-loop	T	C	no	polymorphic site
16193	D-loop	T	C	no	polymorphic site
16221	D-loop	T	C	no	polymorphic site
16523	D-loop	T	C	no	polymorphic site
Analysis of whole mitochondrial genome-11-B4d1a					
73	D-loop	A	G	no	polymorphic site
146	D-loop	T	C	no	polymorphic site
263	D-loop	A	G	no	polymorphic site
750	12S rRNA	A	G	no	polymorphic site
827	12S rRNA	A	G	no	polymorphic site
959	12S rRNA	C	T	no	polymorphic site
1438	12S rRNA	A	G	no	polymorphic site
2706	16S rRNA	A	G	no	polymorphic site
4769	ND2	A	G	no	polymorphic site
7028	COI	C	T	no	polymorphic site
8860	ATPase6	A	G	Thr > Ala	polymorphic site
11719	ND4	G	A	no	polymorphic site
11914	ND4	G	A	no	polymorphic site
12732	ND5	T	C	no	polymorphic site
13942	ND5	A	G	Thr > Ala	polymorphic site
14766	Cytb	C	T	Thr > Ile	polymorphic site
15038	Cytb	A	G	Ile > Val	polymorphic site
15326	Cytb	A	G	Thr > Ala	polymorphic site
15535	Cytb	C	T	no	polymorphic site
16182	D-loop	A	C	no	polymorphic site
16183	D-loop	A	C	no	polymorphic site
16189	D-loop	T	C	no	polymorphic site
16189	D-loop	T	C	no	polymorphic site
16519	D-loop	T	C	no	polymorphic site
16221	D-loop	T	C	no	polymorphic site
16523	D-loop	T	C	no	polymorphic site
Analysis of whole mitochondrial genome-12-B4d1a					
73	D-loop	A	G	no	polymorphic site
146	D-loop	T	C	no	polymorphic site
263	D-loop	A	G	no	polymorphic site
750	12S rRNA	A	G	no	polymorphic site
827	12S rRNA	A	G	no	polymorphic site
959	12S rRNA	C	T	no	polymorphic site
1438	12S rRNA	A	G	no	polymorphic site
2706	16S rRNA	A	G	no	polymorphic site
4769	ND2	A	G	no	polymorphic site
7028	COI	C	T	no	polymorphic site
8860	ATPase6	A	G	Thr > Ala	polymorphic site
11719	ND4	G	A	no	polymorphic site
11914	ND4	G	A	no	polymorphic site
12732	ND5	T	C	no	polymorphic site
13942	ND5	A	G	Thr > Ala	polymorphic site

Supplementary Table 2. Continued

Position	Gene	rCRS Base	Mutation	AA Change	mtDNA Database[a]
14766	Cytb	C	T	Thr > Ile	polymorphic site
15038	Cytb	A	G	Ile > Val	polymorphic site
15326	Cytb	A	G	Thr > Ala	polymorphic site
15535	Cytb	C	T	no	polymorphic site
16182	D-loop	A	C	no	polymorphic site
16183	D-loop	A	C	no	polymorphic site
16189	D-loop	T	C	no	polymorphic site
16189	D-loop	T	C	no	polymorphic site
16519	D-loop	T	C	no	polymorphic site

AA, amino acid; rCRS: revised Cambridge Reference Sequence; mtDNA, mitochondrial DNA; rRNA, ribosomal RNA.
[a]MITOMAP, mtDB, mtSNP, and PhyloTree mt.

Supplementary Table 3. Primers for the Determination of mtDNA Content, mtRNA, Fatty Acid Oxidative, Mitochondrial Translation, Mitophage, Tricarboxylic Acid, and Cholesterol Synthesis

Primer Name	Sequence (5′-3′)
Primers for mtDNA copy number determination	
mt-F3212 / mt-R3319	CACCCAAGAACAGGGTTTGT TGGCCATGGGTATGTTGTTAA
18SF / 18SR	TAGAGGGACAAGTGGCGTTC CGCTGAGCCAGTCAGTGT
Primers for mtRNA determination	
mt-ND1F3310-mt-ND1R3440	CCCATGGCCAACCTCCTACTCCTC AGCCCGTAGGGGCCTACAACG
mt-ND2F4614-mt-ND2R4677	AACCCTCGTTCCACAGAAGCT GGATTATGGATGCGGTTGCT
mt-ND3F10168-mt-ND3R10376	ACGAGTGCGGCTTCGACCCT TCACTCATAGGCCAGACTTAGGGCT
mt-ND4 (L) F10621-mt- ND4 (L) R10694	CCCACTCCCTCTTAGCCAATATT TAGGCCCACCGCTGCTT
mt-ND5F13350-mt-ND5R13426	TGCTCCGGGTCCATCATC TGAGTAGTCCTCCTATTTTTCGAATATCT
mt-ND6F14243-mt-ND6R14439	GCCCCCGCACCAATAGGATCCTCCC CCTGAGGCATGGGGGTCAGGGGT
mt-CO1F6168-mt-CO1R6587	GCCCCCGATATGGCGTTTCCCCGCA GGGGTCTCCTCCTCCGGCGGGGTCG
mt-CO2F7972-mt-CO2R8157	ACCAGGCGACCTGCGACTCCT ACCCCCGGTCGTGTAGCGGT
mt-CO3F9555-mt-CO3R9935	CCCCCAACAGGCATCACCCCGC ATGCCAGTATCAGGCGGCGGC
mt-CYBF15263-mt-CYBR15326	CCCACCCTCACACGATTCTTTA TTGCTAGGGCTGCAATAATGAA
mt-ATP6F8848-mt- ATP6R8910	TTATGAGCGGGCACAGTGATT GAAGTGGGCTAGGGCATTTTT
mt-ATP8F8393-mt- ATP8R8472	CCCACCATAATTACCCCCATACT GGTAGGTGGTAGTTTGTGTTTAATATTTTTAG
18SF/18SR	TAGAGGGACAAGTGGCGTTC CGCTGAGCCAGTCAGTGT
Primers for the determination of fatty acid oxidative genes expression	
CPT1AF / CPT1AR	ATGCGCTACTCCCTGAAAGTG GTGGCACGACTCATCTTGC
CPT1BF / CPT1BR	CCTGCTACATGGCAACTGCTA AGAGGTGCCCAATGATGGGA
VLCADF / VLCADR	TAGGAGAGGCAGGCAAACAGCT CACAGTGGCAAACTGCTCCAGA
MCADF / MCADR	AGAACCTGGAGCAGGCTCTGAT GGATCTGGATCAGAACGTGCCA
SCADF / SCADR	CGGCAGTTACACACCATCTAC GCAATGGGAAACAACTCCTTCTC
ACOX1F / ACOX1R	GGCGCATACATGAAGGAGACCT AGGTGAAAGCCTTCAGTCCAGC
ACLYF / ACLYR	GCTCTGCCTATGACAGCACCAT GTCCGATGATGGTCACTCCCTT
PPARαF / PPARαR	TCGGCGAGGATAGTTCTGGAAG GACCACAGGATAAGTCACCGAG
PGC1αF / PGC1αR	CCAAAGGATGCGCTCTCGTTCA CGGTGTCTGTAGTGGCTTGACT
18SF / 18SR	TAGAGGGACAAGTGGCGTTC CGCTGAGCCAGTCAGTGT
Primers for the determination of mitochondrial translation genes expression	
12S rRNAF / 12S rRNAR	AATAGGTTTGGTCCTAGCCT TGAGGTTTCCCGTGTTGAGT

Supplementary Table 3. Continued

Primer Name	Sequence (5′-3′)
MRPS11F / MRPS11R	CCTTTGCTTCCTGTGGCACAGA GCCTTTCACCACAACTCGGATG
MRPS16F / MRPS16R	GTTGCCCTCAACCTAGACAGGA CCGTTTCCTTCGCAGTCTCTCA
MRPS6F / MRPS6R	CGCTTCCTTATAGGATCTCTGCC GAGACAAGTGCTCCACCATGCT
MRPS22F / MRPS22R	CTACGCAAAGCCTCTTGGGAAG CAACATGCCTGTCCTGGCTATAC
MRPS27F / MRPS27R	CGAGGAAACAGAGCAGTCCAAG ATGTCCTCTGCTTCACAGGTGG
18SF / 18SR	TAGAGGGACAAGTGGCGTTC CGCTGAGCCAGTCAGTGT
Primers for the determination of mitophagy genes expression	
LC3F / LC3R	GCTACAAGGGTGAGAAGCAGCT CTGGTTCACCAGCAGGAAGAAG
P62F / P62R	TGTGTAGCGTCTGCGAGGGAAA AGTGTCCGTGTTTCACCTTCCG
18SF / 18SR	TAGAGGGACAAGTGGCGTTC CGCTGAGCCAGTCAGTGT
Primers for the determination of glycolysis genes expression	
SLC2A1F / SLC2A1R	TTGCAGGCTTCTCCAACTGGAC CAGAACCAGGAGCACAGTGAAG
HK2F / HK2R	GAGTTTGACCTGGATGTGGTTGC CCTCCATGTAGCAGGCATTGCT
GPIF / GPIR	CTGGTAGACGGCAAGGATGTGA TCCGTGATGGTCTTGCCTGTGT
PFKMF / PFKMR	GCTTCTAGCTCATGTCAGACCC CCAATCCTCACAGTGGAGCGAA
PFKLF / PFKLR	AAGAAGTAGGCTGGCACGACGT GCGGATGTTCTCCACAATGGAC
PFKPF / PFKPR	AGGCAGTCATCGCCTTGCTAGA ATCGCCTTCTGCACATCCTGAG
PKMF / PKMR	ATGGCTGACACATTCCTGGAGC CCTTCAACGTCTCCACTGATCG
LDHAF / LDHAR	GGATCTCCAACATGGCAGCCTT AGACGGCTTTCTCCCTCTTGCT
LDHBF / LDHBR	GGACAAGTTGGTATGGCGTGTG AAGCTCCCATGCTGCAGATCCA
Primers for the determination of TCA genes expression	
PDHA1F / PDHA1R	GGATGGTGAACAGCAATCTTGCC TCGCTGGAGTAGATGTGGTAGC
ACO1F / ACO1R	TCCTCAGGTGATTGGCTACAGG TCGGTCAGCAATGGACAACTGG
ACO2F / ACO2R	CAATCGTCACCTCCTACAACAGG GTCTCTGGGTTGAACTTGAGGG
IDH1F / IDH1R	CTATGATGGTGACGTGCAGTCG CCTCTGCTTCTACTGTCTTGCC
IDH2F / IDH2R	AGATGGCAGTGGTGTCAAGGAG CTGGATGGCATACTGGAAGCAG
IDH3AF / IDH3AR	TCGGTGTGACACCAAGTGGCAA TTCGCCATGTCCTTGCCTGCAA
IDH3BF / IDH3BR	TGGCATCTGAGGAGAAGCTGGA TCAGCCGCATATCATAGGAGGC
IDH3GF / IDH3GR	CCAGTGGACTTTGAAGAGGTGC TTTGTGCGACGGTGGCAGGTTA
OGDHF / OGDHR	GAGGCTGTCATGTACGTGTGCA TACATGAGCGGCTGCGTGAACA

Supplementary Table 3. Continued

Primer Name	Sequence (5′-3′)
SUCLA2F / SUCLA2R	GCAAGAAGCTGGTGTCTCCGTT CCACCAGCTAAAACCTGTGCCT
SDHAF / SDHAR	GAGATGTGGTGTCTCGGTCCAT GCTGTCTCTGAAATGCCAGGCA
FHF / FHR	CCGCTGAAGTAAACCAGGATTATG ATCCAGTCTGCCATACCACGAG
MDH1F / MDH1R	CGGTGTCCTAATGGAACTGCAAG CATCCAGGTCTTTGAAGGCAACG
MDH2F / MDH2R	CTGGACATCGTCAGAGCCAACA GGATGATGGTCTTCCCAGCATG
CSF / CSR	CACAGGGTATCAGCCGAACCAA CCAATACCGCTGCCTTCTCTGT
Primers for the determination of cholesterol synthesis genes expression	
CYP51AF / CYP51AR	CTCTTACCAGGTTGGCTGCCTT CTTGAGACTGTCTGCGTTTCTGG
FDFT1F / FDFT1R	TGTGACCTCTGAACAGGAGTGG GCCCATAGAGTTGGCACGTTCT
DHCR24F / DHCR24R	CAGGAGAACCACTTCGTGGAAG CCACATGCTTAAAGAACCACGGC
DHCR7F / DHCR7R	TCCACAGCCATGTGACCAATGC CGAAGTGGTCATGGCAGATGTC
HSD17B7F / HSD17B7R	GCTGATGGACTTCAGGAGGTGT GCACTGCGAGATGATGTCCAGA
NSDHLF / NSDHLR	CAGTTTTCCACTGTGCGTCACC ACGCCCTCAAAGATGACACTGG
HMGCRF / HMGCRR	GACGTGAACCTATGCTGGTCAG GGTATCTGTTTCAGCCACTAAGG
HMGCS1F / HMGCS1R	AAGTCACACAAGATGCTACACCG TCAGCGAAGACATCTGGTGCCA

mtDNA, mitochondrial DNA; mtRNA, mitochondrial RNA.

Supplementary Table 4. Antibodies

Antibodies	Source
Anti-ND1	Proteintech
Anti-ND2	Proteintech
Anti-ND3	Abcam
Anti-ND5	Proteintech
Anti-CYTB	Proteintech
Anti-CO1	Abcam
Anti-CO2	Proteintech
Anti-ATP6	Proteintech
Anti-ATP8	Proteintech
Anti-TOMM20	Proteintech
Anti-GRIM19	Abcam
Anti-SDHA	Abcam
Anti-CORE2	Abcam
Anti-ATP5	Abcam
Anti-GAPDH	Proteintech
Anti-PINK1	Proteintech
Anti-CLPP	Proteintech
Anti-LONP1	Proteintech
Anti-AFG3L2	Proteintech
Anti-HSP60	Proteintech
Anti-GRP75	Proteintech
Anti-ACTIN	Proteintech
Anti-RXRA	Abcam
Anti-NRF1	Abcam
Anti-JNK1/2	Cell Signaling Technology
Anti-P-JNK1/2	Cell Signaling Technology
Anti-p38	Cell Signaling Technology
Anti-phospho-p38 (Thr389)	Cell Signaling Technology
Anti-ERK1/2	Cell Signaling Technology
Anti-phospho-ERK (Thr202/Tyr204)	Cell Signaling Technology
Anti-AKT1	Cell Signaling Technology
Anti-P-AKT (Thr473)	Cell Signaling Technology
Anti-AMPKα	Cell Signaling Technology
Anti-P- AMPKα	Cell Signaling Technology
Anti-CPT1A	Abcam
Anti-ACOX1	Abcam
Anti-PPARα	Abcam
Anti-ABCA1	Proteintech
Anti-ABCG5	Proteintech
Anti-ABCG8	Proteintech
Anti-CYP7A1	Proteintech
Anti-HIF1α	Proteintech
Anti-HIF2α	Proteintech
Anti-HMGCR	Proteintech

References

1. Miquel JFG, Covarrubias C, Villaroel L, Mingrone G, Greco AV, Puglielli L, Carvallo P, Marshall G, Del Pino G, Nervi F. Genetic epidemiology of cholesterol cholelithiasis among Chilean Hispanics, Amerindians, and Maoris. Gastroenterology 1998;115:937–946.
2. de Saint Pierre M, Bravi CM, Motti JM, Fuku N, Tanaka M, Llop E, Bonatto SL, Moraga M. An alternative model for the early peopling of southern South America revealed by analyses of three mitochondrial DNA haplogroups. PLoS One 2012;7:e43486.
3. Moro PL, Checkley W, Gilman RH, Cabrera L, Lescano AG, Bonilla JJ, Silva B. Gallstone disease in Peruvian coastal natives and highland migrants. Gut 2000;46:569–573.
4. Brandini S, Bergamaschi P, Cerna MF, Gandini F, Bastaroli F, Bertolini E, Cereda C, Ferretti L, Gomez-Carballa A, Battaglia V, Salas A, Semino O, Achilli A, Olivieri A, Torroni A. The Paleo-Indian Entry into South America According to Mitogenomes. Mol Biol Evol 2018; 35:299–311.
5. Brasca AP, Pezzotto SM, Berli D, Villavicencio R, Fay O, Gianguzzo MP, Poletto L. Epidemiology of gallstone disease in Argentina: prevalences in the general population and European descendants. Dig Dis Sci 2000; 45:2392–2398.
6. Bobillo MC, Zimmermann B, Sala A, Huber G, Rock A, Bandelt HJ, Corach D, Parson W. Amerindian mitochondrial DNA haplogroups predominate in the population of Argentina: towards a first nationwide forensic mitochondrial DNA sequence database. Int J Legal Med 2010;124:263–268.
7. Everhart JE, Khare M, Hill M, Maurer KR. Prevalence and ethnic differences in gallbladder disease in the United States. Gastroenterology 1999;117:632–639.
8. Kumar S, Bellis C, Zlojutro M, Melton PE, Blangero J, Curran JE. Large scale mitochondrial sequencing in Mexican Americans suggests a reappraisal of Native American origins. BMC Evol Biol 2011;11:293.
9. Maurer KR, Everhart JE, Ezzati TM, Johannes RS, Knowler WC, Larson DL, Sanders R, Shawker TH, Roth HP. Prevalence of gallstone disease in Hispanic populations in the United States. Gastroenterology 1989;96:487–492.
10. Zhang W, Ng HW, Shu M, Luo H, Su Z, Ge W, Perkins R, Tong W, Hong H. Comparing genetic variants detected in the 1000 genomes project with SNPs determined by the International HapMap Consortium. J Genet 2015;94:731–740.
11. Gonzalez Villalpando C, Rivera Martinez D, Arredondo Perez B, Martinez Diaz S, Gonzalez Villalpando ME, Haffner SM, Stern MP. High prevalence of cholelithiasis in a low income Mexican population: an ultrasonographic survey. Arch Med Res 1997;28:543–547.
12. Green LD, Derr JN, Knight A. mtDNA affinities of the peoples of North-Central Mexico. Am J Hum Genet 2000;66:989–998.
13. Lai SW, Ng KC. Risk factors for gallstone disease in a hospital-based study. South Med J 2002; 95:1419–1423.
14. Chen CH, Huang MH, Yang JC, Nien CK, Etheredge GD, Yang CC, Yeh YH, Wu HS, Chou DA, Yueh SK. Prevalence and risk factors of gallstone disease in an adult population of Taiwan: an epidemiological survey. J Gastroenterol Hepatol 2006; 21:1737–1743.
15. Chen YC, Chiou C, Lin MN, Lin CL. The prevalence and risk factors for gallstone disease in taiwanese vegetarians. PLoS One 2014;9:e115145.
16. Li YC, Tian JY, Liu FW, Yang BY, Gu KSY, Rahman ZU, Yang LQ, Chen FH, Dong GH, Kong QP. Neolithic millet farmers contributed to the permanent settlement of the Tibetan Plateau by adopting barley agriculture. Natl Sci Rev 2019;6:1005–1013.
17. Sun H, Tang H, Jiang S, Zeng L, Chen EQ, Zhou TY, Wang YJ. Gender and metabolic differences of gallstone diseases. World J Gastroenterol 2009; 15:1886–1891.
18. Gu Q, Zhou G, Xu T. Risk factors for gallstone disease in Shanghai: An observational study. Medicine 2020;99: e18754.
19. Song ST, Shi J, Wang XH, Guo YB, Hu PF, Zhu F, Zeng X, Xie WF. Prevalence and risk factors for gallstone disease: A population-based cross-sectional study. J Dig Dis 2020;21:237–245.
20. Zhang FM, Yu CH, Chen HT, Shen Z, Hu FL, Yuan XP, Xu GQ. Helicobacter pylori infection is associated with gallstones: Epidemiological survey in China. World J Gastroenterol 2015;21:8912–8919.
21. Xu P, Yin XM, Zhang M, Liang YJ. Epidemiology of gallstone in Nanjing City in China. Zhonghua Liu Xing Bing Xue Za Zhi 2004;25:928.
22. Zhu L, Aili A, Zhang C, Saiding A, Abudureyimu K. Prevalence of and risk factors for gallstones in Uighur and Han Chinese. World J Gastroenterol 2014; 20:14942–14949.
23. Nomura H, Kashiwagi S, Hayashi J, Kajiyama W, Ikematsu H, Noguchi A, Tani S, Goto M. Prevalence of gallstone disease in a general population of Okinawa, Japan. Am J Epidemiol 1988;128:598–605.
24. Kim SB, Kim KH, Kim TN, Heo J, Jung MK, Cho CM, Lee YS, Cho KB, Lee DW, Han JM, Kim HG, Kim HS. Sex differences in prevalence and risk factors of asymptomatic cholelithiasis in Korean health screening examinee: A retrospective analysis of a multicenter study. Medicine 2017;96:e6477.
25. Lee HY, Yoo HE, Park MJ, Chung U, Kim CY, Shin KJ. East Asian mtDNA haplogroup determination in Koreans: haplogroup-level coding region SNP analysis and subhaplogroup-level control region sequence analysis. Electrophoresis 2006;27:4408–4418.
26. Prathnadi P, Miki M, Suprasert S. Incidence of cholelithiasis in the northern part of Thailand. J Med Assoc Thai 1992;75:462–470.
27. Shaffer EA. Epidemiology and risk factors for gallstone disease: has the paradigm changed in the 21st century? Curr Gastroenterol Rep 2005;7:132–140.
28. Kutanan W, Kampuansai J, Srikummool M, Kangwanpong D, Ghirotto S, Brunelli A, Stoneking M. Complete mitochondrial genomes of Thai and Lao

populations indicate an ancient origin of Austroasiatic groups and demic diffusion in the spread of Tai-Kadai languages. Hum Genet 2017;136:85–98.
29. Attili AF, Carulli N, Roda E, Barbara B, Capocaccia L, Menotti A, Okoliksanyi L, Ricci G, Capocaccia R, Festi D, et al. Epidemiology of gallstone disease in Italy: prevalence data of the Multicenter Italian Study on Cholelithiasis (M.I.COL.). Am J Epidemiol 1995; 141:158–165.
30. Khan HN, Harrison M, Bassett EE, Bates T. A 10-year follow-up of a longitudinal study of gallstone prevalence at necropsy in South East England. Dig Dis Sci 2009;54:2736–2741.
31. Gyedu A, Adae-Aboagye K, Badu-Peprah A. Prevalence of cholelithiasis among persons undergoing abdominal ultrasound at the Komfo Anokye Teaching Hospital, Kumasi, Ghana. Afr Health Sci 2015; 15:246–252.
32. Heinz T, Pala M, Gomez-Carballa A, Richards MB, Salas A. Updating the African human mitochondrial DNA tree: Relevance to forensic and population genetics. Forensic Sci Int Genet 2017;27:156–159.
33. Safer L, Bdioui F, Braham A, Ben Salem K, Soltani MS, Bchir A, Saffar H. Epidemiology of cholelithiasis in central Tunisia. Prevalence and associated factors in a nonselected population. Gastroenterol Clin Biol 2000; 24:883–887.
34. Unisa S, Jagannath P, Dhir V, Khandelwal C, Sarangi L, Roy TK. Population-based study to estimate prevalence and determine risk factors of gallbladder diseases in the rural Gangetic basin of North India. HPB (Oxford) 2011;13:117–125.
35. Massarrat S. Prevalence of gallstone disease in Iran. J Gastroenterol Hepatol 2001;16:564–567.
36. Derenko M, Malyarchuk B, Bahmanimehr A, Denisova G, Perkova M, Farjadian S, Yepiskoposyan L. Complete mitochondrial DNA diversity in Iranians. PLoS One 2013;8:e80673.
37. Volzke H, Baumeister SE, Alte D, Hoffmann W, Schwahn C, Simon P, John U, Lerch MM. Independent risk factors for gallstone formation in a region with high cholelithiasis prevalence. Digestion 2005;71:97–105.
38. FamilyTreeDNA, Available at: https://www.familytreedna.com/, Accessed February 18, 2016.